

**THE EFFECTS OF *TULBAGHIA VIOLACEA*
LEAF, BULB AND STALK EXTRACTS ON
JURKAT CELLS**

Jared Stuart Mackenzie (208502480)

2012

**Submitted in fulfilment of the requirements for the degree of
Master of Medical Sciences in
Discipline of Medical Biochemistry
School of Medical Sciences
School of Laboratory Medicine and Medical Sciences
College of Health Sciences
University of KwaZulu Natal
Durban
South Africa**

ABSTRACT

Studies have shown that the traditional healers have used *Tulbaghia violacea* (TV) (also known as 'wild garlic') for the treatment of a number of ailments including fever, tuberculosis, stomach problems, and oesophageal cancer. However, little is known with regards to the anticancer and antiproliferative properties of this plant. Therefore, this study investigated the effects of TV and domesticated garlic extracts on Jurkat cells, in order to determine whether or not these extracts possess anti-proliferative properties. Cultured Jurkat cells were treated with IC₅₀ concentrations of garlic (14µg/ml), TV leaf (256µg/ml), TV bulb (225µg/ml) and TV stalk (216µg/ml) extracts as determined by the methylthiazol tetrazolium assay. Free radical production was measured using the thiobarbituric acid reactive substance (TBARS) and nitric oxide (NO) assays, while glutathione (GSH) concentration was measured using the GSH-Glo™ assay. The apoptosis inducing properties of each extract were measured using flow cytometry (Annexin V- Fluos and JC-1 assays) and luminometry (caspases 3/7, 8, 9 and ATP). Western blots were run to determine protein expression, while comet and DNA fragmentation assays were used to determine the level of DNA damage induced. Wild and domesticated garlic extracts induced a significant increase in malondialdehyde concentration ([MDA]), with TV bulb extract inducing the highest concentration (p<0.0001). A significant increase in NO concentration was observed in the bulb (p<0.0001) and stalk (p<0.001) extracts, and leaf (p<0.05) and stalk (p<0.05) TV extracts significantly increasing GSH concentration. The longest comet tails were observed in TV bulb extracts (p<0.0001) and comprised mainly of single strand breaks, while the comets induced following garlic exposure contained double strand breaks. All extracts, except TV leaf, increased the percentage of cells undergoing apoptosis. *Tulbaghia violacea* leaf induced a significant (p<0.0001) increase in percentage of cells

undergoing necrosis, whereas TV bulb resulted in a significant ($p < 0.0001$) decrease. All TV extracts induced caspase 3/7 and 9 activity, with the most significant increase in caspase 9 activity observed for TV leaf and bulb. No significant change in caspase 3/7 activity was evident for domesticated garlic. Cleavage of PARP and expression of NF κ B and HSP 70 occurred for all extracts. However, HSP 70 was not differentially expressed. Exposure to wild and domesticated garlic extracts induced peroxidative lipid and DNA damage within the cells, indicating oxidative stress. This damage occurred in conjunction with increased percentage of cells undergoing apoptosis and expression of caspase 3/7. Therefore, these findings suggest that TV is inducing cell death through apoptosis in Jurkat cells using a number of mechanisms, including the induction of oxidative stress. This is of clinical significance, as cell death through apoptosis is the preferred method of action for anti-cancer drugs.

DECLARATION

I, Jared Stuart Mackenzie, hereby declare that this thesis entitled

“The effect of *Tulbaghia violacea* leaf, bulb and stalk extracts on Jurkat cells”

is the result of my own investigation and research and that it has not been submitted in part or in full for any other degree or to any other university. Where use was made of the work of others, it is duly acknowledged in the text.

Date: _____

J.S. Mackenzie

ACKNOWLEDGEMENTS

The financial assistance of the National Research Foundation (NRF) towards this research is hereby acknowledged. The opinions expressed and conclusions arrived at in this thesis are those of the author and are not necessarily attributed to the NRF. I would like to thank my supervisors Rene Myburg and Metse Serumula for their help, support and encouragement for the duration of the study, as well as thank Kogi Moodley for her help throughout the study, specifically during the extraction process. I would also like to thank Prof. A.A. Chuturgoon for his encouragement and guidance throughout the study, and acknowledge all who assisted me and provided me with support in the Discipline of Medical Biochemistry. I would like to make special mention of Ms A Phulukdaree who assisted me by performing the flow and luminometry aspects of this study.

I would like to thank my family and friends, who supported me and provided encouragement whenever it was needed.

PUBLICATIONS

The following paper is to be submitted to the Journal of Ethnopharmacology:

Mackenzie, J., Moodley, K., Mackraj, I., Chaturgoon, A., Serumula, M and Myburg, R. (2012). Tulbaghia violacea leaf, bulb and stalk extracts induce cell death in Jurkat cells. *Ethnopharmacology*.

The following paper is to be submitted to the Journal of Traditional, Complementary and Alternative Medicine:

Mackenzie, J., Moodley, K., Mackraj, I., Chaturgoon, A., Serumula, M and Myburg, R. (2012). Tulbaghia violacea leaf, bulb and stalk extracts induce oxidative stress in Jurkat cells. *The Journal of Traditional, Complementary and Alternative Medicine*.

ABBREVIATIONS

·OH	Hydroxyl radical
[MDA]	Malondialdehyde concentration
1O_2	Singlet oxygen
ACE	Angiotensin Converting Enzyme
AIF	Apoptosis inducing factor
AKT	Protein kinase B
ANOVA	One –way analysis of variance
APAF	Apoptotic protease activating factor
ATF	Activating transcription factor
ATP	Adenosine Tri-Phosphate
BCA	Bicinchoninic acid
BHT	Butylhydroxytoluene
BSA	Bovine Serum Albumin
CAMs	Complementary and alternative medicines
CAT	Catalase
CCM	Complete Culture Medium
CNS	Central nervous system
COX	Cyclooxygenase
DMSO	Dimethyl sulfoxide
ERK1/2	Extracellular signal-regulated kinases 1 and 2
EtBr	Ethidium Bromide
GPx	Glutathione peroxidase
GSH	Glutathione
GSSG	Glutathione disulphide

H₂O₂	Hydrogen peroxide
HNE	4-hydroxy-2-nonenal
HSP	Heat shock protein
	inositol polyphosphate 5' phosphatase
Itk	IL2-inducible T-cell kinase
LMPA	Low Melting Point Agarose
LPS	Lipopolysaccharide
MAPK	Mitogen-activated protein kinase
MDA	Malondialdehyde
MDA	Malondialdehyde
MTT	Methylthiazol tetrazolium
NEDD	<i>N</i> -1-naphthylethylenediamine dihydrochloride
NFκB	Nuclear factor κB
NO	Nitric Oxide
O₂⁻	Superoxide anion radical
PARP	Poly (ADP-ribose) Polymerase
PBMCs	Peripheral blood mononuclear cells
PBS	Phosphate Buffered Saline
PI3K	Phosphoinositide- 3- kinase
PTEN	Phosphatase and Tension homologue
PUFA	Polyunsaturated fatty acid
RLU	Relative Light Units
RNS	Reactive Nitrogen Species
ROS	Reactive Oxygen Species
SCGE	Single cell gel electrophoresis

SHIP	SH2 - domain - containing
SOD	Superoxide dismutase
SULF	Sulphanilamide
TBARS	Thiobarbituric Acid Reactive Substance
Th1	Type 1 Helper cells
Th2	Type 2 Helper cells
TNF	Tumor Necrosis Factor
TTBS	Tris-Buffered Saline and Tween 20
TV	<i>Tulbaghia violacea</i>
UV	Ultraviolet
VCl₃	Vanadium Chloride
WHO	World Health Organisation

LIST OF FIGURES

CHAPTER 2		Page number:
Figure 1	Sources of ROS and its role in cancer development, adapted from Waris & Ahsan (2006).	10
Figure 2	Chain propagation in lipid peroxidation showing the initiation, propagation and termination steps (Catalá, 2009).	12
Figure 3	The antioxidant action of mitochondrial superoxide dismutase, GSH peroxidase and catalase.	18
Figure 4	Diagram showing the metabolism of alliin (Amagase, 2006).	21
Figure 5	<i>Tulbaghia violacea</i> A) Whole plant and B) Flowers (Lyantagaye, 2011)	22
Figure 6	Chemical structure of Allicin (Oommen <i>et al.</i> , 2004)	23
Figure 7	Chemical structure of Ajoene (Dirsch <i>et al.</i> , 1997)	24
CHAPTER 3		
Figure 8	Images used to determine visual scoring of comets following fluorescent microscopy (Collins, 2004).	35
CHAPTER 4		
Figure 9	MTT curves showing % cell viability for A) Garlic, B) TV Leaf, C) TV Bulb and D) TV Stalk	45
Figure 10	The malondialdehyde (MDA) concentration in Jurkat cells	46

following treatment with garlic and *Tulbaghia violacea* extracts. All treatments caused a dramatic increase in MDA concentration. The samples were run in triplicate, with the assay performed 3 times to validate data. ** $p < 0.001$, and *** $p < 0.0001$ by comparison with the control group

- Figure 11** The Nitric Oxide (NO) concentration in Jurkat cells following treatment with garlic and *Tulbaghia violacea* extracts. Only TV bulb and TV stalk treatment resulted in a significant increase in NO concentrations. The assay was performed twice to validate data ** $p < 0.001$, and *** $p < 0.0001$ by comparison with the control group. 47
- Figure 12** The Glutathione (GSH) concentration in Jurkat cells following treatment with garlic and *Tulbaghia violacea* extracts. Only TV leaf and TV bulb resulted in a significant increase in GSH concentration * $p < 0.05$ by comparison with the control group. 48
- Figure 13** Fluorescent microscope images of Jurkat cells (following treatment with garlic and *Tulbaghia violacea* extracts) showing DNA fragmentation, indicated by the “comet” like appearance of the cells. According to these illustrations, garlic appears to have the most potent effect as seen by the almost total disappearance of the nucleus. A) Control, B) Garlic, C) TV Leaf, D) TV Bulb, and E) TV Stalk (magnification= 400x). 50

- Figure 14** The comet tail length in Jurkat cells following treatment with garlic and *Tulbaghia violacea* extracts. All extracts resulted in an increase in comet tail length, with the greatest increase seen following treatment with TV bulb. *** $p < 0.0001$ by comparison with the control group **50**
- Figure 15** DNA fragmentation in Jurkat cells following treatment with garlic and *Tulbaghia violacea* extracts. A) 1.8% gel, B) 2% gel. The 1.8% gel shows double and single strand breaks, whereas the 2% gel shows laddering DNA fragmentation. The positive control contained 50 μ M camptothecin, whereas the negative control contained normal DNA obtained from A549 cells. **52**
- Figure 16** The percentage of living, apoptotic, and necrotic Jurkat cells following treatment with garlic and *Tulbaghia violacea* extracts. A) % Living cells, B) % Cells undergoing apoptosis. All extracts, except TV leaf, resulted in a significant increase in % cells undergoing apoptosis. C) % Cells undergoing necrosis. TV leaf induced a significant increase in % cells undergoing necrosis, whereas TV bulb resulted in a significant decrease. *** $p < 0.0001$ by comparison with the control group. **54**
- Figure 17** The caspase concentration A) Caspase 3/7, B) Caspase 8, and C) Caspase 9 in Jurkat cells following treatment with garlic and *Tulbaghia violacea* extracts. TV extracts increased caspase **56**

3/7 expression and TV leaf and bulb significantly increased caspase 9 expression. Domesticated garlic had no significant effect on caspase expression. * $p < 0.05$ and ** $p < 0.001$ by comparison with the control group.

- Figure 18** The percentage depolarisation following treatment with garlic and *Tulbaghia violacea* extracts. TV stalk induced a significant increase in % depolarisation. All other extracts resulted in no significant change. * $p < 0.05$ by comparison with the control group. 57
- Figure 19** The ATP concentration in Jurkat cells following treatment with garlic and *Tulbaghia violacea* extracts. TV leaf was the only extract to induce a significant increase in ATP concentration. * $p < 0.05$ by comparison with the control group. 58
- Figure 20** Coomassie Blue stain of SDS PAGE gel following protein extraction 59
- Figure 21** Western blot analyses of apoptotic molecules in Jurkat cells. Isolated proteins were subjected to western blot analyses with the respective antibodies. Cleavage of PARP and expression of NF κ B, HSP 70 and β – actin was seen following treatment with all extracts. A) Cleaved PARP bands (89Kd and 24Kd), B) NF κ B, C) HSP 70, D) β – actin 60

APPENDIX

Figure 22	Standard curve used in order to determine and standardise protein concentration in western blots	93
Figure 23	Standard curve used to determine NO concentration.	93
Figure 24	Relative Band Density for all treatments, including the control, after performing a western blot analysis. A) PARP 89 KD, and B) PARP 24 KD. Values are presented as Means \pm SD, where the columns represent means, and the vertical lines represent SD. * $p < 0.05$ and ** $p < 0.001$ by comparison with the control group.	95
Figure 25	Relative Band Density for all treatments, including the control, after performing a western blot analysis. A) NFκB, B) HSP 70, and C) Beta actin. Values are presented as Means \pm SD, where the columns represent means, and the vertical lines represent SD.	96

LIST OF TABLES**CHAPTER 4**

Table 1	IC50 values obtained for each extract following an MTT assay	45
Table 2	Visual score of “comets” following treatment with extracts. ***p<0.0001 by comparison with the control group.	51
Table 3	Summary table showing a summary of all the data for each extract	61

APPENDIX

Table 4	Individual comet visual scores following an SCGE assay.	94
----------------	--	-----------

TABLE OF CONTENTS

	Page number:
ABSTRACT	i
DECLARATION	iii
ACKNOWLEDGEMENTS	iv
PUBLICATIONS	v
ABBREVIATIONS	vi
LIST OF FIGURES	ix
LIST OF TABLES	xiv
TABLE OF CONTENTS	xv
CHAPTER 1: INTRODUCTION	1
CHAPTER 2: LITERATURE REVIEW	4
2.1. The Immune system	4
2.2. Cancer	4
2.2.1. Free radicals.	6
2.2.2. Lipid Peroxidation	11
2.2.3. DNA oxidation	14
2.2.4. Antioxidants	14
2.3. Conventional cancer treatment	18
2.3.1. Complementary and Alternative Medicines (CAMs)	19
2.3.1.1. Garlic	19
2.3.1.2. <i>Tulbaghia violacea</i> (wild garlic)	21

2.4. Cell Model – Jurkat cells	25
2.5. Hypothesis	26

CHAPTER 3: MATERIALS AND METHODS

3.1. Materials	27
3.2. Methods	27
3.2.1. <i>Tulbaghia violacea</i>	27
3.2.2. Extraction process	28
3.2.3. Cell culture	28
3.2.4. Methylthiazol tetrazolium (MTT) assay	29
3.2.5. Thiobarbituric Acid Reactive Substances (TBARS) assay	30
3.2.6. Nitric Oxide	32
3.2.7. Glutathione (GSH) determination	32
3.2.8. Single Cell Gel Electrophoresis (SCGE) Assay	33
3.2.9 DNA fragmentation	35
3.2.10. Annexin V – Fluos.	37
3.2.11. Caspase determination.	37
3.2.12. JC – 1 Assay	38
3.2.13. ATP determination	39
3.2.14. Western blots	40
3.2.15. Coomassie Blue Staining	42
3.2.16. Data Analysis	43

CHAPTER 4: RESULTS	
4.1. General	44
4.2. MTT assay	44
4.3. TBARS Assay	46
4.4. Nitric Oxide Assay	47
4.5 GSH..	48
4.6. SCGE Assay.	49
4.7. DNA Fragmentation.	51
4.8. Annexin V – Fluos.	52
4.9. Caspase activation.	55
4.10. JC – 1 assay	57
4.11. ATP expression	58
4.12. Coomassie staining	59
4.13. Western Blots	59
CHAPTER 5: DISCUSSION	62
CHAPTER 6: CONCLUSION	71
REFERENCES	73
APPENDICES	85
Appendix A	85
Appendix B	86

Appendix C	87
Appendix D	88
Appendix E	89
Appendix F	90
Appendix G	92
Appendix H	93

CHAPTER 1

INTRODUCTION

Cancer is a disease that has afflicted mankind since time immemorial. The global cancer burden has increased tremendously in recent decades (Auyang, 2004). In the year 2008, 12.7 million new cancer cases were diagnosed, with 7.6 million deaths attributed to cancer world-wide (Center *et al.*, 2011). The World Health Organisation (WHO) estimated that if this trend were to continue, annual global cancer deaths could increase to 15 million by 2020 (Auyang, 2004).

Chronic inflammation represents one of the potential mechanisms by which cancer could develop (Aggarwala *et al.*, 2006). This is attributed to the overproduction of reactive oxygen species (ROS), reactive nitrogen species (RNS) and inflammatory cytokines which lead to macromolecule damage (Zhang, 2011). Humans have developed an active antioxidant system (glutathione (GSH), catalase, superoxide dismutase (SOD) etc) to overcome the potentially damaging effects of these ROS (Fiaschi & Chiarugi, 2012). Oxidative stress results when increased ROS overwhelm the antioxidant capacity to detoxify them, contributing to the development and progression of cancer (Fiaschi & Chiarugi, 2012).

The conventional forms of treatment recommended for cancer by physicians include aggressive medical, radiation and surgical therapies (Valdivieso, *et al.*, 2012). However, conventional treatment has limited success and studies now show that an increasing number of cancer patients are declining conventional treatment and opting for complementary and alternative medicines (CAM) instead (Verhoef *et al.*, 2008)

(Molassiotis *et al.*, 2005). This appears to be due to the side effects often associated with chemotherapy.

In all forms of cancer treatments, the preferred method of action is through altering cell proliferation or inducing cytotoxic activity within the cells (Bungu *et al.*, 2006). This reduced proliferation can be due to cell death mechanisms such as apoptosis. Studies have shown that this form of cell death results in decreased activation of the immune system, as cell destruction is more specific/localised (Tang *et al.*, 2008). Apoptosis can occur through the extrinsic pathway, intrinsic pathway, or both (Tang *et al.*, 2008). The extrinsic pathway is triggered by the Fas death receptor, and results in the activation of caspase 8, and eventually caspase 3 which cleaves PARP resulting in apoptosis (Tang *et al.*, 2008). The intrinsic pathway results in the release of cytochrome c, which leads to the activation of caspase 9 and 3 (Tang *et al.*, 2008). These begin the caspase cascade, and lead to apoptosis.

Although CAMs have been shown to be beneficial in the treatment of a variety of illnesses, further studies need to be conducted on these CAMs in order to determine the mechanisms by which they exert their effects, as well as their efficacy and safety. Medicinal plants form part of CAMs, one that is of great interest is garlic (*Allium sativum*). It has been used for many years by traditional healers as a herbal remedy to treat various ailments such as infections, diarrhoea, heart disease, and diabetes (Aviello *et al.*, 2009). Further clinical studies have revealed that it exerts antilipidemic, antihypertensive, antibacterial, antineoplastic and hypoglycaemic actions (Aviello *et al.*, 2009).

Tulbaghia violacea (TV) or 'wild garlic' is a medicinal plant that is indigenous to the Eastern Cape of South Africa, and is believed to have similar properties to garlic (Bungu *et al.*, 2006). Traditionally, the leaves are eaten as vegetables (Bungu *et al.*, 2006). However, the leaves and bulbs of TV have also been used by traditional healers to treat various ailments, including fever, tuberculosis, stomach problems, and oesophageal cancer (Bungu *et al.*, 2006). As this medicinal plant has not been comprehensively studied, its previous use by traditional healers and the relatively recent finding that it possesses similar properties to garlic has caused great interest in the scientific world. As a result, its use in the treatment of cancer warrants further investigation (Auyang, 2004).

Therefore, the following research questions were addressed:

- 1) Do TV and domesticated garlic extracts induce cell death in the Jurkat cells?
- 2) By which mechanisms do these extracts act?
- 3) Which plant components have the most profound effect?

CHAPTER 2

LITERATURE REVIEW

2.1 The immune system

The immune system is required by the body in order to maintain homeostasis through protection from invading pathogens (Sompayrac, 2008). It is a very complex system and is made up of a number of cells, barriers, and tissues that work together in order to protect the body from disease (Sompayrac, 2008). Its main function is to identify pathogens or foreign material, and remove these from the body (Farmer & Packard, 1986). This system is divided into both the innate and adaptive immune systems (Sompayrac, 2008). However, these both rely on each other and each plays a vital role.

Normal functioning of the immune system is vital for survival. There are various factors which can affect its functioning, resulting in the development of a number of diseases. In some cases, these factors can result in uncontrolled cell proliferation which can lead to disease such as cancer, which is of particular interest for this study.

2.2 Cancer

Cancer is a disease that has afflicted mankind for many centuries. However, its prevalence has increased drastically in recent times (Auyang, 2004). It is defined as “a group of diseases characterised by unregulated division and spread of abnormal cells” (Auyang, 2004).

Most cancers develop within various tissues in the form of a tumour (Auyang, 2004). The location in which they originally develop classifies them into the various types (Auyang, 2004). These include lung, colon, breast, prostate, skin and brain cancer. However, the proliferative ability of cancer cells allows them to divide and spread (metastasis) (Auyang, 2004). Metastasis occurs when cancerous cells proliferate at an accelerated rate and migrate from the primary tumor (Ramaswamy *et al.*, 2003). They are able to survive in the blood or lymphatic circulation and invade other tissues within the body where they can establish a secondary tumour (Ramaswamy *et al.*, 2003). The cancer cells have thus, through invasion of the blood system and other tissues, resulted in the establishment of new 'colonies' (Auyang, 2004).

There have been various hypotheses regarding the cause of cancer. A prominent hypothesis is the formation of malignant tumours due to genetic abnormalities that have been shown to account for 5-10 percent of reported breast and colon cancer cases world - wide (Auyang, 2004). Studies have shown that genetic defects in DNA repair, DNA damage check-points, and telomere maintenance may predispose to cancer (Brown & Attardi, 2005).

One such defect that has been described is a mutation in the tumour suppressor protein p53 (Brown & Attardi, 2005). The normal function of this protein is to protect the genome, causing cell cycle arrest or apoptosis upon detection of stresses such as DNA damage and hypoxia (Brown & Attardi, 2005). As a result, its mutation can lead to uncontrolled proliferation of cells, thereby aiding cancer formation (Brown & Attardi, 2005).

Sporadic or non-inherited cancers account for the vast majority of cancer cases (Auyang, 2004). Causes include environmental factors such as exposure to pollution, radiation

(natural and artificial) and chemicals. A poor diet and working conditions, as well as exposure to viruses and bacteria have also been shown to have an affect on cancer development (Auyang, 2004). Studies have shown that smoking and obesity account for roughly 45 percent of all cancer deaths in the United States (Auyang, 2004).

These factors have been shown to induce cancer formation through the development of chronic inflammation (Aggarwala *et al.*, 2006). Smoking, as well as exposure to pollution and viruses can result in chronic inflammation. Studies have shown that, although inflammation can assist in the removal of pathogens, it also appears to have various oncogenic properties (Grivennikov *et al.*, 2010). It has been shown to result in the overproduction of reactive oxygen species (ROS), reactive nitrogen species (RNS), and inflammatory cytokines (Zhang, 2011). This excess production of ROS and RNS can lead to oxidative stress and DNA damage.

2.2.1. Free radicals

According to Valko *et al.*,(2007), “Free radicals can be defined as molecules or molecular fragments containing one or more unpaired electrons in atomic or molecular orbitals.” This property makes these free radicals more reactive (and unstable) than “non-radicals” (Tudek *et al.*, 2010). Reactive oxygen species exist normally within all aerobic cells of the body and are most commonly derived through the metabolism of oxygen (Waris & Ahsan, 2006). However, they can also develop as a result of certain diets, during inflammatory reactions (released by neutrophils) and following exposure to ultraviolet (UV) radiation (Tudek *et al.*, 2010).

The process of obtaining adenosine triphosphate (ATP) through aerobic metabolism is dependent on a process known as oxidative phosphorylation that occurs within the mitochondria (Thannickal & Fanburg, 2000). Oxygen is required as it acts as the final electron acceptor for cytochrome C oxidase (electron transfer reaction) (Thannickal & Fanburg, 2000). Cytochrome C oxidase catalyses the conversion of O_2 to H_2O , a process whereby metabolites of oxygen may be formed (Thannickal & Fanburg, 2000). Electrons generated during electron transfer react with oxygen to form free radicals such as superoxide (Nordberg & Arner, 2001). Superoxide acts to form hydrogen peroxide, whereas catalase acts to form water and oxygen from hydrogen peroxide (Nordberg & Arner, 2001) (Scibior & Czczot, 2006).

The main ROS that are formed include the superoxide anion radical (O_2^-), singlet oxygen (O_2^{\bullet}), hydrogen peroxide (H_2O_2), and the hydroxyl radical ($\cdot OH$) (Waris & Ahsan, 2006). However, the main source of ROS comes from H_2O_2 and O_2^- . (Waris & Ahsan, 2006) (Valko *et al.*, 2007).

Superoxide can be produced from oxygen through various pathways. These include the oxidation of NADPH by NADPH oxidase, as well as the oxidation of xanthine or hypoxanthine. Reduction reactions such as the reduction of O_2 by cytochrome P_{450} can also result in the formation of O_2^{\bullet} (Fang *et al.*, 2002). Hydrogen peroxide can be produced through two electron reduction by Cytochrome P_{450} (Fang *et al.*, 2002).

Studies have shown that ROS play a role in intracellular signaling (Waris & Ahsan, 2006). In particular, they are involved in the pathways that regulate cell growth and

differentiation.(Valko *et al.*, 2007). This agrees with the findings of Thannickal & Fanburg, who showed that ROS are involved in TNF and IL-1 mediated apoptosis (Thannickal & Fanburg, 2000). However, ROS are usually viewed as harmful metabolic by-products.

In certain cases, excessive stimulation of NADPH or a dysfunction in the mitochondrial electron transport chain can result in an overproduction of ROS (Valko *et al.*, 2007). This can result in the development of oxidative stress. Reduced antioxidant production has also been found to be a major cause of oxidative stress (Valko *et al.*, 2007). This process can result in various negative effects within the body, and has been shown to be a mediator of cell damage (Valko *et al.*, 2007). Excessive ROS production has been shown to cause tissue damage by reacting with lipids found in cell membranes, nucleotides that make up cellular DNA, and sulphydryl groups in proteins (Waris & Ahsan, 2006).

Reactive nitrogen species are another form of oxidants that develop within cells (Devasagayam *et al.*, 2004). These oxidants are derived from nitric oxide (NO) and include nitrogen dioxide (NO₂), peroxynitrite (ONOO⁻), nitrosoperoxycarbonate (ONOOCO₂⁻) and S-nitrosothiols (Nash *et al.*, 2012); (Martínez & Andriantsitohaina, 2009). Peroxynitrite is produced during a reaction between NO and O₂ - and is said to be the most active RNS (Walker *et al.*, 2001).

These oxidants play various important roles within the body and are necessary for the regulation of a number of cellular processes. However, as with ROS, high levels of RNS

can result in various negative effects such as the development of oxidative stress and can induce damage through oxidation, nitration and nitrosylation (Nash *et al.*, 2012).

Studies have shown that oxidative stress can cause oxidation of amino acid residue side chains found in proteins, with cysteine and methionine residues being particularly susceptible to oxidation (Valko *et al.*, 2007). This can lead to the formation of disulphides and low molecular weight thiols (Valko *et al.*, 2007).

DNA damage induced by oxidative stress can result in the development of various mutations. The majority of these mutations involve guanine modifications, in particular, transversions of guanine to thymine (Waris & Ahsan, 2006). According to Valko *et al.* oxidative stress can also result in increased oxidation of phospholipids (lipid peroxidation). This can lead to the development of peroxy radicals, and eventually production of malondialdehyde (MDA) (Valko *et al.*, 2007).

As oxidative stress has been shown to cause tissue damage through various mechanisms, it is believed to be partly responsible for the development of a number of human diseases. Studies have shown that it plays a role in the development of cancer, diabetes, atherosclerosis, pulmonary fibrosis, neurodegenerative diseases, and aging (Thannickal & Fanburg, 2000) (Waris & Ahsan, 2006).

Of particular interest for this study is the role of oxidative stress in the development of cancer. As mentioned previously, oxidative stress has been shown to induce various changes and mutations within DNA. These include modification of DNA bases, gene duplications, rearrangement of the DNA sequence, and activation of oncogenes (Waris

& Ahsan, 2006). These changes and mutations can affect the cell cycle and induce proliferation, apoptosis, and senescence; all of which are involved in cancer development (Figure 1) (Waris & Ahsan, 2006). According to Valko *et al.* studies have shown that cancer cells often present with a cellular redox imbalance when compared to normal cells (Valko *et al.*, 2007). This supports the theory that oxidative stress may be implicated in cancer development.

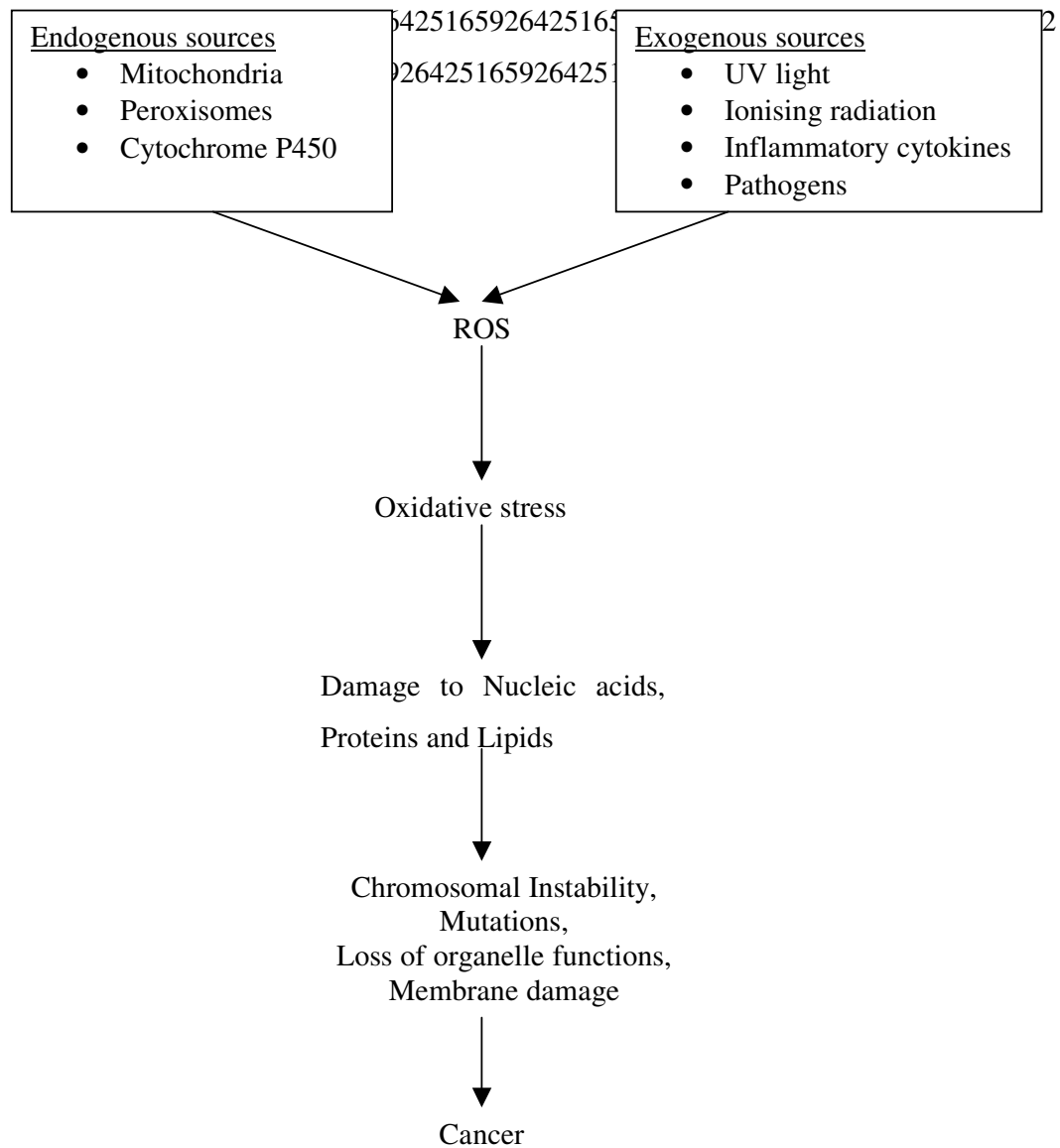


Figure 1: Sources of ROS and its role in cancer development (Waris & Ahsan, 2006)

2.2.2. Lipid Peroxidation

Lipid peroxidation occurs when ROS remove a hydrogen atom from an unsaturated fatty-acyl chain (Fang *et al.*, 2002). This results in an unpaired electron on the carbon (radicals) of the fatty-acyl chain. These radicals react with oxygen to produce peroxy radicals that are able to oxidise membrane proteins and attack adjacent side chains (Halliwell, 2006). This begins a chain reaction resulting in more carbon atoms with unpaired electrons, as well as peroxy radicals, and eventually cyclic peroxides (Halliwell, 2006).

Peroxy radicals undergo various reactions, including the decomposition of phospholipids hydroperoxide, until malondialdehyde (MDA) and 4-hydroxy-2-nonenal (HNE) (products of peroxidation) remain. (Catalá, 2009, Valko *et al.*, 2007). This process is known as chain propagation (Figure 2) and consists of initiation, propagation and termination steps (Fang *et al.*, 2002).

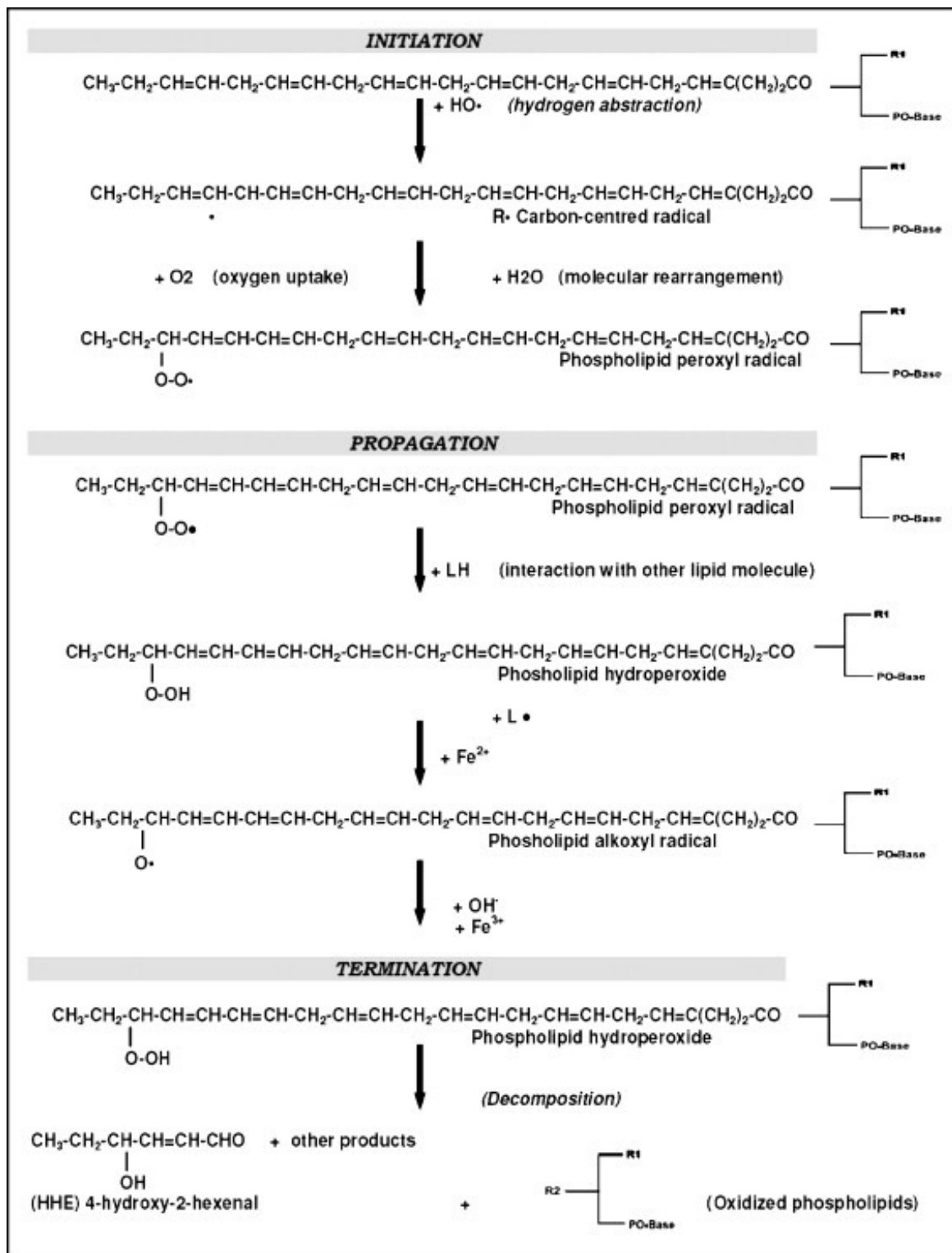


Figure 2: Chain propagation in lipid peroxidation showing the initiation, propagation and termination steps (Catalá, 2009).

Malondialdehyde is not only a product of lipid peroxidation, but is also generated during prostaglandin biosynthesis (Marnett, 2002). Marnett (2002) showed that MDA reacts with DNA to form various adducts. An adduct is defined as “a complex formed by the chemical binding of a foreign substance (usually cancer causing) to DNA” (Neher & Stürzenbaum, 2006). These adducts can result in “miscoding,” and can therefore be responsible for the development of various mutations within cells (Tudek *et al.*, 2010). As a result, DNA adducts formed due to lipid peroxidation are said to be good predictive biomarkers for cancer (Tudek *et al.*, 2010).

The other product of lipid peroxidation (HNE) acts as a mediator of oxidative stress, and has been extensively studied for its possible contribution towards cancer development (Pizzimenti *et al.*, 2010). Due to its electrophilic properties, HNE reacts with glutathione, proteins and DNA (Pizzimenti *et al.*, 2010). It is also involved in the regulation of various processes, such as signal transduction, cell proliferation and differentiation (Pizzimenti *et al.*, 2010). As with MDA, the interaction between HNE and DNA results in the formation of DNA adducts (Pizzimenti *et al.*, 2010).

The effects of lipid peroxidation result in decreased membrane fluidity and increased membrane permeability (Halliwell, 2006). It also results in the inactivation of receptors and enzymes and can cause damage to membrane proteins (Halliwell, 2006).

2.2.3. DNA Oxidation

Research has shown that DNA oxidation can result in damage to all 4 DNA bases, as well as the deoxyribose sugar. This includes nucleotide modifications, particularly in sequences high in guanine content (Bennett, 2001).

The hydroxyl radical has been shown to react with DNA resulting in strand breakage through the process of β -cleavage (Aust & Eveleigh, 1999). This radical can also alter DNA base pairs through the addition of double bonds and the abstraction of hydrogen atoms from methyl groups (Aust & Eveleigh, 1999). Peroxynitrite is another oxidant that reacts directly with guanine base pairs in DNA, thereby altering their structure and making them further susceptible to oxidation (Aust & Eveleigh, 1999). This DNA damage induced by oxidants can occur in a number of cells, including macrophages and can result in apoptosis (Bennett, 2001).

2.2.4. Antioxidants

In order to protect against the deleterious effects of ROS, cells have developed various defence mechanisms. These defence mechanisms include preventative mechanisms, repair mechanisms, physical defences, and antioxidant defences (Valko *et al.*, 2007). The main function of these antioxidants is to scavenge free radicals and prevent oxidative stress (Valko *et al.*, 2007). Antioxidant defence mechanisms involve the use of antioxidants, as well as antioxidant enzymes, both of which work together to scavenge free radicals (Valko *et al.*, 2007).

The main antioxidants include glutathione (GSH), arginine, citrulline, taurine, creatine, selenium, zinc, alpha - tocopherol (vitamin E), ascorbic acid (vitamin C), vitamin A, and tea polyphenols (Fang *et al.*, 2002). Whereas the main antioxidant enzymes involved include superoxide dismutase (SOD), catalase (CAT), glutathione reductase, and glutathione peroxidase (Fang *et al.*, 2002).

Vitamin E acts as a lipid soluble, non-enzymatic antioxidant. Its main function is to reduce lipid peroxidation through the transfer of a hydrogen atom to a peroxidized polyunsaturated fatty acid (PUFA) (or peroxy radical) (Fang *et al.*, 2002). This transfer interrupts chain propagation, thereby preventing peroxidation of PUFA within membrane phospholipids (Fang *et al.*, 2002). Vitamin E is therefore known as a “chain breaking antioxidant” (Burton & Traber, 1990). Its production is regulated by vitamin C and GSH activity (Burton & Traber, 1990, Valko *et al.*, 2007). However, it can also be obtained directly through food intake (Burton & Traber, 1990).

Vitamin C is a water soluble, non-enzymatic antioxidant. Studies have shown that it actively scavenges ROS and RNS, and plays a role in the regeneration of other antioxidants (Carr & Frei, 1999). These include vitamin E, GSH, urate, and β – carotene (Carr & Frei, 1999). According to Carr & Frei, vitamin C is a highly effective antioxidant, and can be regenerated through various pathways (Carr & Frei, 1999). Like vitamin E, this antioxidant can also be obtained through diet (Carr & Frei, 1999).

Glutathione is synthesised from glutamate, cysteine and glycine and is said to be an exogenous and endogenous antioxidant (Fang *et al.*, 2002). Within the cell, GSH is distributed throughout the nuclei, cytosol and mitochondria (Valko *et al.*, 2007). In the

nucleus, GSH is also required for the functioning of various DNA repair mechanisms (Valko *et al.*, 2007).

Along with the activation of DNA repair mechanisms, GSH also acts as a cofactor for glutathione peroxidase, scavenges ROS directly, and is involved in the regulation of various other important antioxidants, such as vitamins C and E (Valko *et al.*, 2007). Glutathione peroxidase acts as a potent antioxidant enzyme, and catalyses the reduction of H_2O_2 to H_2O (Thannickal & Fanburg, 2000). Glutathione peroxidase is also required for the detoxification of precursors of lipid peroxidation (lipid hydroperoxides), resulting in the formation of alcohol (Figure 5) (Fang *et al.*, 2002).

According to Fang *et al.* the main ROS targeted by GSH include the lipid peroxy radical, peroxynitrite, and H_2O_2 (Fang *et al.*, 2002). Following oxidation, GSH is converted to glutathione disulphide (GSSG) (Valko *et al.*, 2007). The ratio of GSH to GSSG is often used as a measure of oxidative stress within the body (Valko *et al.*, 2007). Approximately 90% of cells contain GSH in its reduced form (Kidd, 1997). As GSH is an important antioxidant, its deficiency could result in various abnormalities. For example, a deficiency in GSH has been shown to be a contributory factor to liver damage, and lung disease in smokers (Kidd, 1997).

Another important antioxidant is the enzyme superoxide dismutase (SOD). This is part of a family of metalloenzymes and the “first line of defence” against ROS (Alscher *et al.*, 2002). It is divided into three main types (Turrens, 2003). These include cytosolic Cu/ZnSOD (SOD1), mitochondrial MnSOD (SOD2) and extracellular SOD (ecSOD or SOD3) (Gongora *et al.*, 2006). These SODs are involved in maintaining low levels of

O_2^\bullet , by catalysing the conversion of O_2^\bullet to O_2 and H_2O_2 (Turrens, 2003) (Fang *et al.*, 2002) (Figure 3).

Catalase (Figure 3) is also an antioxidant enzyme that works in association with glutathione peroxidase to catalyse the reduction of H_2O_2 to H_2O and O_2 within peroxisomes (Cao *et al.*, 2003). In order for this reaction to take place, catalase requires the presence of NADPH (Fang *et al.*, 2002). Catalase is also required for the detoxification of lipid peroxides, resulting in the formation of non-toxic alcohol (Olorunnisola *et al.*, 2012). As studies have shown that H_2O_2 is implicated in the induction of apoptosis, catalase is believed to be involved in the prevention of apoptosis, due to its ability to reduce hydrogen peroxide to water and oxygen (Cao *et al.*, 2003, Matsura *et al.*, 1999).

Antioxidants act to combat ROS, thereby leading to reduced DNA damage. As DNA damage has been implicated in the development of cancer, various drugs have brought about much interest as anti-cancer agents due to the presence of antioxidant properties.

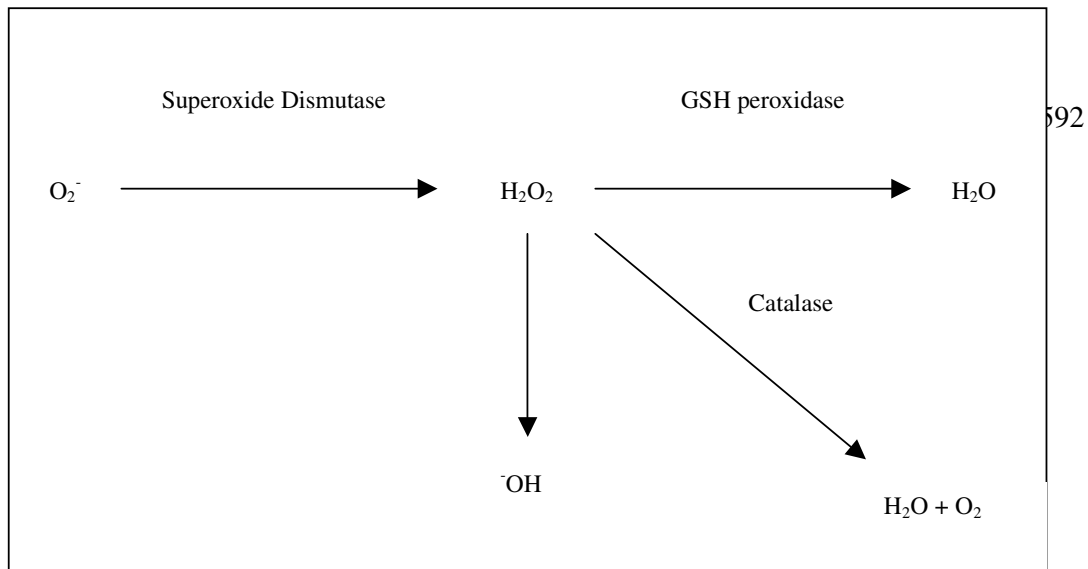


Figure 3: The antioxidant action of mitochondrial superoxide dismutase, GSH peroxidase and catalase.

2.3. Conventional cancer treatment

The conventional forms of treatment recommended for cancer by physicians include aggressive medical, radiation and surgical therapies (Valdivieso, *et al.*, 2012). In the case of leukaemia, patients often receive radiation therapy in conjunction with normal chemotherapy (Sinks, 1972). This additional treatment is believed to help prevent the development of central nervous system (CNS) leukaemia (Sinks, 1972). Central nervous system leukaemia develops when leukaemic cells are present within the CNS, and is diagnosed by the presence of blast cells in a sample of cerebrospinal fluid (CSF) (Gribbni, 1977). The chemotherapy is given in high doses, or administered directly into the CSF where it is able to reach the CNS (Sinks, 1972). In all forms of cancer treatments, the preferred method of action is through altering proliferation of the

cancerous cells or inducing cytotoxicity (apoptosis) within the cells (Bungu *et al.*, 2006).

Although conventional treatment has been successful in the past, studies have shown that an increasing number of cancer patients are declining conventional treatment, and are using complementary and alternative medicines (CAM) instead (Verhoef *et al.*, 2008). Research has shown that 70.2% of cancer patients make use of CAMs (Molassiotis *et al.*, 2005). The main reason for this appears to be due to patients having a negative experience with conventional medicine (Verhoef *et al.*, 2008). However, loss of family members or friends while on conventional treatment also appears to play a part (Verhoef *et al.*, 2008).

2.3.1. Complementary and alternative medicines (CAMs)

Studies have shown that cancer patients using CAM therapies appear to use a wide range of treatments , rather than focusing on just one (Cassileth, 1999). The most commonly used therapies include “dietary treatments, herbal remedies, homeotherapy, hypnotherapy, imagery/visualisation, meditation, megavitamins, relaxation and spiritual healing” (Cassileth, 1999). Dietary supplements and herbal remedies account for roughly 20% of CAMs used by cancer patients (Cassileth, 1999).

2.3.1.1. Garlic

One such dietary treatment that is of great interest is garlic (*Allium sativum*). Commercially, it is used in cooking in order to add flavour to food (Aviello *et al.*, 2009). However, it has also been used for many years by traditional healers as a herbal

remedy to treat various ailments such as infections, diarrhoea, heart disease, and diabetes (Aviello *et al.*, 2009). Further experimental studies have revealed that it appears to exert antilipidaemic, antihypertensive, antibacterial, antineoplastic and hypoglycaemic actions (Aviello *et al.*, 2009).

Of particular interest to this study is the antineoplastic action of garlic. Aviello *et al.* (2009) have suggested various mechanisms through which garlic may act to reduce the spread and development of cancer. These include activation of apoptosis, and reduced cell proliferation via its effects on the cell cycle (Aviello *et al.*, 2009). It has also been found to inhibit cyclooxygenase (COX)-2 expression and acts as an antioxidant (enhances glutathione – S – transferase activity), thereby reducing the number of circulating free radicals (Aviello *et al.*, 2009).

The chemical constituents of garlic are divided into both sulphur- and non - sulphur containing compounds (Aviello *et al.*, 2009). Most of the cancer protective effects attributed to garlic are due to the sulphur containing compounds, in particular allicin (Dorant *et al.*, 1993). This compound is formed from alliin in a reaction catalysed by allinase (Figure 3) when garlic is chopped or crushed (Aviello *et al.*, 2009, Oommen *et al.*, 2004). Garlic has also been found to be rich in arginine, and is therefore able to suppress inflammation (Milner, 2006). Cancer development has previously been shown to occur due to chronic inflammation (Aggarwala *et al.*, 2006). Therefore, anti-inflammatory agents such as garlic are able to reduce cancer risk.

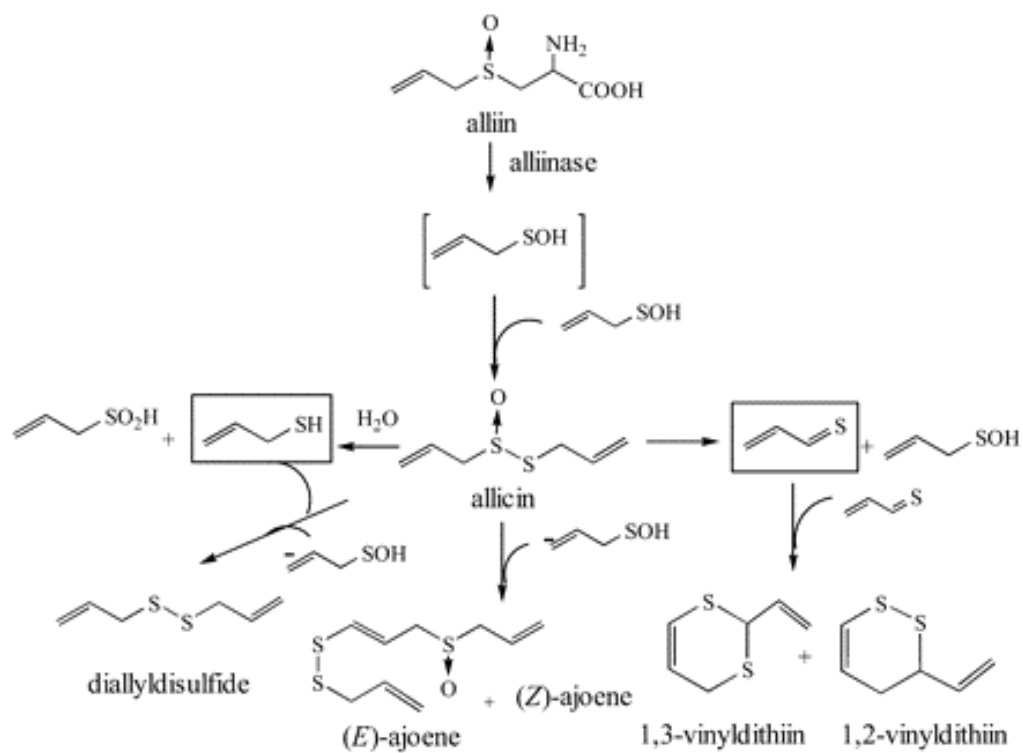


Figure 4: Diagram showing the metabolism of alliin (Amagase, 2006).

2.3.1.2. *Tulbaghia violacea* (Wild Garlic)

Tulbaghia violacea (Figure 5) is a plant that is indigenous to the Eastern Cape of South Africa, and is believed to have similar properties to garlic (Bungu *et al.*, 2006). However, the medicinal properties of this plant have not been as extensively studied as domesticated garlic, and for this reason it is of great interest (Bungu *et al.*, 2008).

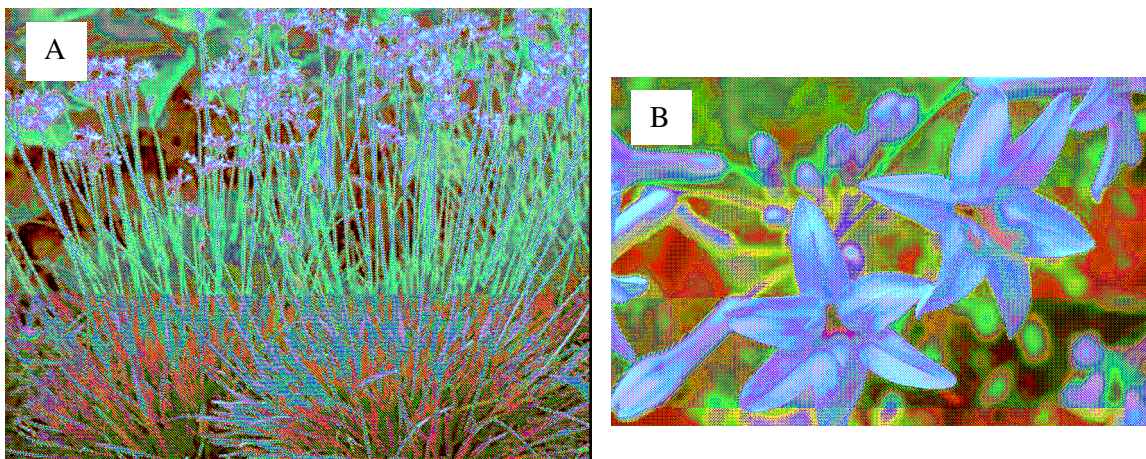


Figure 5: *Tulbaghia violacea* A) Whole plant and B) Flowers (Lyantagaye, 2011).

Traditionally, the leaves of this plant are eaten as vegetables (Bungu *et al.*, 2006). However, the leaves and bulbs of *T. violacea* have also been used by traditional healers to treat various ailments, including fever, tuberculosis, stomach problems, and oesophageal cancer (Bungu *et al.*, 2006). These extracts have been suggested to be involved in the inhibition of angiotensin converting enzyme (ACE) (Bungu *et al.*, 2006). As a result, they may prove useful in the treatment of hypertension.

Garlic has been shown to have anti-proliferative properties through the inhibition of cancer cell proliferation and induction of apoptosis (Zaid *et al.*, 2011). These properties are thought to be due to the presence of a number of organosulphur compounds found in garlic (Zaid *et al.*, 2011). However, Bungu *et al* (2006) have shown that similar sulphur compounds have been discovered in *T. violacea*. As a result, this has brought about much interest regarding the possible anti-cancer properties of *T. violacea* as it is beneficial for anti cancer drugs to act through the inhibition of cell proliferation (Bungu *et al.*, 2006).

As in commercial garlic, *T. violacea* also contains allicin (Oommen *et al.*, 2004) (Figure 4, 6). Studies conducted by Patya *et al.* have shown that allicin presents with both immunostimulatory and antitumour properties (Patya *et al.*, 2004). Allicin plays a role in the control of the various biological actions of ferrocene (synthetic iron-containing compound) (Patya *et al.*, 2004).

Patya *et al.*, (2004) also found that activation of extracellular signal-regulated kinases 1 and 2 (ERK1/2) within human peripheral mononuclear cells and wild type Jurkat T-cells occurred following administration of allicin. As ras (a GTPase) is downstream of the ERKs, it has been suggested that P21ras is the main target of allicin (Patya *et al.*, 2004). It is through the activation of this protein that allicin induces the activation of lymphocytes (Patya *et al.*, 2004).

Following its formation from alliin, allicin is rapidly metabolised to various other sulphur compounds (Oommen *et al.*, 2004). These include diallyl sulphide, diallyl disulfide, diallyl trisulfide, ajoene, S-allylmer captocysteine, S-allyl cysteine and vinyl dithiines (Oommen *et al.*, 2004) (Figure 4).

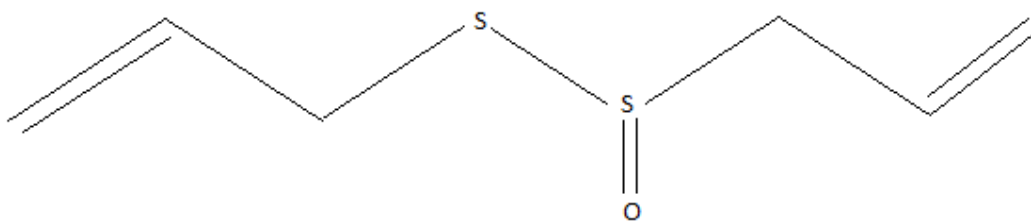


Figure 6: Chemical structure of allicin (Oommen *et al.*, 2004).

Ajoene [(*E*, *Z*)-4,5,9-trithiadodeca-1, 6,11-triene-9-oxide] (Figures 4, 7) is formed following the metabolism of allicin. This compound is found in both commercial garlic,

as well as *T. violacea*, and has also been extensively studied for its medicinal properties (Dirsch *et al.*, 1997). Studies conducted by Dirsch *et al.* showed that ajoene appears to induce apoptosis within human leukaemia cells, but not within peripheral blood mononuclear cells (PBMCs) of healthy donors (Dirsch *et al.*, 1997). They postulated that this occurs through the stimulation of peroxides, production of reactive oxygen species (ROS), as well as the activation of nuclear factor kB (NFkB) (Dirsch *et al.*, 1997).

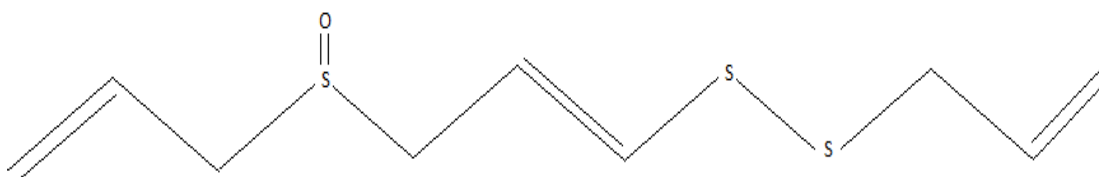


Figure 7: Chemical structure of ajoene (Dirsch *et al.*, 1997).

Tulbaghia violacea has been found to contain various antioxidant properties, and is therefore often used in the management of free radicals. It is also used in the management of diseases that develop due to oxidative stress (Olorunnisola *et al.*, 2012).

In a study conducted by Olorunnisola *et al.* it was shown that oral administration of methanolic extracts of *T. violacea* rhizome in rats resulted in a dose dependent increase in the activities of SOD, CAT and glutathione peroxidase (GPx) with a corresponding decrease in lipid peroxidation (Olorunnisola *et al.*, 2012).

This decrease in lipid peroxidation may also be due to the presence of polyphenolic compounds within the extract in addition to the increased antioxidant activity

(Olorunnisola *et al.*, 2012). However, studies have also shown that organosulphur compounds (ajoene) found within *T. violacea* may in fact result in an increase in ROS production within certain cell types (e.g. tumourigenic cells) thereby inducing apoptosis (Dirsch *et al.*, 1997, Kay *et al.*, 2010).

In order to conduct the present study, and determine whether or not the use of *T. violacea* is a viable option for the treatment of diseases such as cancer, a cell model is needed.

2.4. Cell Model - Jurkat cells

Most cancers occur as solid tumours within tissues. However, in some cases, cancer can develop within the blood. When this occurs, it is known as leukaemia. There are various different types of leukaemia, including T-cell leukaemia, lymphoid leukaemia and acute nonlymphoblastic leukaemia (Shah *et al.*, 2008).

Studies have shown that in Great Britain alone, over 400 cases of leukaemia are diagnosed each year (Shah *et al.*, 2008). In South Africa, leukaemia accounts for 25.4% of all cancers seen in children (Stefan & Stones, 2012). As a result, the need for the development of new forms of cancer treatment is of great importance.

In the present study a leukaemia cell line known as Jurkat was used. Jurkat cells (originally designated JM) are an immortalised T-lymphocyte cell line established in the late 1970's from the peripheral blood of a 14-year old boy with T-cell leukaemia (Bartelt *et al.*, 2009). They are used because they have retained their ability to produce

interleukin-2 (Bartelt *et al.*, 2009). However, they are also routinely used to determine mechanisms of cancer susceptibility to drugs and radiation (Bartelt *et al.*, 2009). Jurkat cells are very useful in that they grow quickly, are easy to culture, and provide a useful model for studying acute T-cell leukaemia (Bartelt *et al.*, 2009).

2.5. Hypothesis

Conventional cancer treatments, although relatively effective, can be very toxic and dangerous to the patient (Verhoef *et al.*, 2008). With more and more people resorting to CAMs, the need for a safer and more natural means of treatment is of great importance. Much research has been previously undertaken on garlic and its antiproliferative properties. As a result, the relatively recent finding of the organosulphur compounds present in *T. violacea* could be of vital importance. The easy availability of this plant, and its common use in traditional medicine makes it an attractive prospect for cancer patients. Therefore, the aim of this study was to determine the effects of TV extracts (Bulb, Leaf and stalk) on Jurkat cells (an immortalised leukaemic T- cell line) in an effort to determine whether or not these extracts possess anti-cancer properties through the inhibition of cancer cell proliferation or the induction of cancer cell cytotoxicity. These morphological parts of the plant were chosen as previous studies have focused on the effects of TV bulb and leaf on cancerous cell lines other than Jurkat cells (Bungu *et al.*, 2006). Since no research has previously been conducted on TV stalk in a cancerous cell line, this study also investigated the effect of TV stalk extract on the Jurkat cells.

CHAPTER 3

MATERIALS AND METHODS

3.1. Materials

All tissue culture consumables were purchased from Whitehead Scientific (Johannesburg, South Africa) and the Jurkat cells were purchased from Highveld Biological (Johannesburg, South Africa). The methylthiazol tetrazolium (MTT) salt, phosphate buffered saline (PBS) tablets, thiobarbituric acid (TBA), butylated hydroxytoluene (BHT), malondialdehyde (MDA), all reagents required for the nitric oxide (NO) assay, bicinchoninic acid (BCA) assay kit, ethidium bromide and agarose were purchased from Capital Laboratory Supplies (Johannesburg, South Africa). Kits and reagents used for luminometry (GSH-Glo™ Glutathione Assay kit, Caspase-Glo® 3/7,9 and 8 assay kits) and flow cytometry (Annexin V-Fluos and JC-1) were purchased from Promega (USA) and BD Biosciences (USA), respectively. Western blotting reagents (Laemmli sample buffer and LumiGLO chemiluminescent reagent) were procured from BioRad. The primary antibodies (anti-NFκB, anti-PARP and anti-HSP70) and horse-radish peroxidase (HRP)-conjugated secondary antibodies (anti-rabbit IgG and anti-goat IgG) were purchased from Sigma. All other solvents and salts were purchased from Merck Chemicals (Johannesburg, South Africa).

3.2. Methods

3.2.1. *Tulbaghia violacea*

Tulbaghia violacea (Dry mass = 501.62g) was harvested and authenticated by Professor H. Baijnath (Department of Biological Sciences, UKZN). The bulb, leaf and stalk sections were separated and washed thoroughly with water and left to dry for 48 hours

at room temperature. The dry weight of each plant portion was then determined (TV bulbs= 200.35g, TV leaves= 185g and TV stalks= 116.27g).

3.2.2. Extraction process

The dry plant was blended to a pulp in methanol using a commercial blender (Waring Products Division, Dynamics Corporation of America, New Hartford, Connecticut). Blending was aided through the addition of methanol (TV Bulbs = 200ml, TV Leaves = 500ml and TV stalks = 260ml) and the active components extracted in additional methanol (Bulbs = 300ml, Leaves = 500ml, Fleshy stalk = 240ml) for 48 hours, as previously shown by Bungu *et al.*, 2006. Active components have previously been found by Bungu *et al.*, 2006. After 48hours, each mixture was filtered twice using a Büchner funnel (Haldenwanger, Berlin) and filter paper (Whatman International LTD Maidstone, England). The filtrates were then left to stand for 24 hours to allow for the evaporation of methanol under a laminar flow hood. A rotary evaporator (Genevac LTD, Ipswich, England) was used to remove the remainder of the methanol from the extracts. The optimum temperature required for the evaporation of methanol for all 3 extracts ranged between 79°C and 85°C.

3.2.3. Cell culture

Jurkat cells were cultured in suspension (± 2 million cells /75cm³ culture flask (30000 cells/ml)) and maintained in 10% complete culture medium (CCM: RPMI 1640, supplemented with 10% foetal calf serum, 1% penstrep fungizone and 1% L-glutamine). Foetal calf serum was added as it supplies the cells with growth factors. Penstrep

fungizone is an antibiotic that was added in order to prevent microbial contamination. L-glutamine was added to promote culture development and to be used for protein production and as an energy source. The cells were incubated in a humidified incubator at 37°C (5% CO₂). The media was replaced and cells counted following a change in media colour from red to orange/yellow (indicating that the cells were metabolising) (usually about every 48hrs). The media was changed by centrifuging the cells at 1491rpm at 24°C for 10 minutes. The supernatant was then discarded and replaced with fresh media.

A Cell count was performed by adding 150µl CCM and 50µl trypan blue to 50µl cell suspension. Next, 20µl of this solution was loaded onto a haemocytometer with a cover slip placed on top. The cells were then counted using an inverted microscope, and the number of cells per millilitre determined using the following equation:

$$\text{Cell number} = \text{Average cell number} \times \text{dilution factor} (5) \times 10^4 \text{ cells}$$

3.2.4. Methylthiazol tetrazolium (MTT) assay

The MTT assay is a colorimetric assay that was performed in order to determine the viability of treated cells, as well as the half-maximal inhibitory concentrations (IC₅₀) for each extract. In this assay, viable cells convert MTT (cleaved by mitochondria) to formazan crystals, thereby determining mitochondrial dehydrogenase enzyme activity (Mosmann, 1983, Van Meerloo *et al.*, 2011). MTT is also converted to formazan within the cytosol, through accepting electrons from substrates such as NADH and NADPH (Vistica *et al.*, 1991). The amount of formazan generated is proportional to the number

of living cells (Mosmann, 1983). This assay is normally used to determine the cytotoxic effects of drugs on cell lines (Van Meerloo *et al.*, 2011).

The cells (4×10^4 , 150 μ l) were treated with varying concentrations of each extract in triplicate (150 μ l CCM was used for the control) in a 96 well microtitre plate to obtain final test concentrations that ranged from 0 – 250 μ g/ml. The treated cells were then incubated at 37°C (5% CO₂) for 24 hours. Following the incubation period, the cells were centrifuged (1491rpm for 10 min at 24°C) (centrifuge 5804R, Hamberg, Germany), and the supernatant removed. Next, 100 μ l of CCM and 20 μ l of MTT salt (5mg/ml in PBS) was added to the cell pellet, and incubated for a further 4 hours. The cells were centrifuged, and the supernatant removed as before. Dimethyl sulfoxide (DMSO) (100 μ l) was then added to solubilise the formazan. Following 1-hour incubation at 37°C, the absorbance was determined using a Bio-Tek μ Quant MQx200 spectrophotometer (South Africa) at a wavelength of 570nm and a reference wavelength of 690nm. The IC₅₀ value for each extract was determined using GraphPad Prism (Version 5) and then used in subsequent assays (Garlic= 14 μ g/ml, TV leaf= 256 μ g/ml, TV bulb= 225 μ g/ml, TV stalk= 216 μ g/ml). For all subsequent assays the cells were incubated with the IC₅₀ concentration of each extract for 24 hours

3.2.5. Thiobarbituric Acid Reactive Substances (TBARS) assay

Lipid peroxidation occurs when ROS remove a hydrogen atom from an unsaturated fatty-acyl chain (Fang *et al.*, 2002). One of the by-products of lipid hydroperoxides is malondialdehyde (MDA), which is able to react with thiobarbituric acid (TBA) (Valko

et al., 2007). Butylhydroxytoluene (BHT) is added to prevent oxidation. During this reaction, a coloured product forms which can be measured spectrophotometrically.

This assay was performed in triplicate in order to determine the level of lipid peroxidation within the cells following treatment with wild and domesticated garlic. All reagents were prepared according to the protocol in appendix A. The concentration of MDA was measured within the cells. The treated cells (1×10^5) were centrifuged and the supernatant removed. The pellets were resuspended in the CCM (500 μ l) and homogenised by passing them through a 27-gauge needle 25 times. Positive (1 μ l MDA) and negative (100 μ l CCM) controls were then prepared. Next, 2% H₃PO₄ (200 μ l) and 7% H₃PO₄ (400 μ l) was added to each sample tube. This was followed by the addition of 400 μ l TBA/BHT (with the exception of the negative control) and 200 μ l 1M HCl to each test tube. All tubes were then heated at 100°C for 15 minutes, and allowed to cool to room temperature. After cooling, 1.5ml butanol was added to each test tube, which was then vortexed and allowed to settle into two distinct layers. The top layer (100 μ l) was pipetted (in triplicate) into a 96 well plate and read using a Bio-Tek MQx200 spectrophotometer (South Africa) at 532nm, with a reference wavelength of 600nm. The concentrations of MDA within the samples and controls were then determined using the following equation:

$$[MDA](M) = \text{average absorbance} / 156mM * 1000$$

3.2.6. Nitric Oxide

Nitric oxide production was determined through the measurement of NO^{2-} under acidic conditions using the Griess Reagent system. Nitric oxide levels were measured as an indirect indicator of RNS in the cell (Tarpey *et al.*, 2004). The nitrate is reduced by vanadium and then detection of the NO^{2-} is by the acidic Griess reaction (Fidan *et al.*, 2009).

All reagents were prepared according to the protocol in appendix B. The sample (1×10^5 cells/treatment 50 μl) was added in triplicate to the wells of a 96 well microtitre plate. Sodium nitrite standards were also prepared (0 μM - 200 μM) and 50 μl of each was added in triplicate to the wells. This was followed by the rapid addition of 50 μl vanadium chloride (VCl_3), 25 μl 2% sulphanilamide (SULF) and 50 μl 0.1% *N*-1-naphthylethylenediamine dihydrochloride (NEDD). The plate was then incubated (37°C) for 45 minutes in the dark, and the optical density read at 540/690nm using a spectrophotometer (Bio-Tek MQx200, South Africa). A standard curve (Appendix H) was constructed using the results obtained from the nitrite standards and the resultant NO concentration for each sample was determined by extrapolation.

3.2.7. Glutathione (GSH) determination

The principle of this assay is based on a reaction whereby a luciferin derivative is converted into luciferin by glutathione S-transferase in the presence of GSH (Murphy *et al.*, 2008). The signal generated is proportional to the amount of glutathione present in the sample (Murphy *et al.*, 2008).

The GSH assay (Luminometry) was performed according to the manufacturers' instructions and required the treated cells (1×10^4 cells) to be suspended in 50 μ l PBS and transferred to a luminometry plate in triplicate. Along with the samples, standards were also added in triplicate to the plate. The 2x GSH-GloTM reagent (50 μ l) was added to each sample and standard. This was then mixed briefly on a plate shaker, followed by an incubation period at room temperature for 30 minutes in the dark. After the incubation period, 100 μ l of luciferin detection reagent was added to each sample, and then mixed using a plate shaker. The plates were then incubated in the dark for 15 minutes and read on a ModulusTM microplate luminometer (Turner Biosystems, Sunnyvale, USA). A standard curve was constructed and the concentration of GSH for the treated samples was determined by extrapolation.

3.2.8. Single Cell Gel Electrophoresis (SCGE) Assay

A SCGE (or comet) assay was performed in order to detect DNA strand breaks in eukaryotic cells. This is an alkaline based assay whereby the cells are lysed to form nucleoids containing supercoiled loops of DNA linked to the nuclear matrix (Collins, 2004). Electrophoresis results in comet like structures as the DNA is being pulled away from the nucleus towards the anode (Collins, 2004). A large comet tail and small nucleus indicates a large number of DNA breaks (Collins, 2004).

This assay was performed following the protocol used by (Singh *et al.*, 1988) with minor modifications. All reagents were prepared according to the protocol in appendix C. Briefly, the first gel layer (1% Low Melting Point Agarose (LMPA) at 37°C) was

pipetted (400 μ l) onto the frosted end of a microscope slide, covered with coverslips and refrigerated at 4°C for 10 minutes. After the 10 minutes, the coverslips were removed and a second gel layer (0.5% LMPA at 37°C) was prepared by adding 25 μ l cell suspension (~20 000 cells/treatment) to 175 μ l of LMPA (37°C). From this eppendorf, 200 μ l was removed and placed onto the first layer to form the second gel layer. The coverslips were replaced, and the slides were allowed to solidify as before. After refrigeration, the coverslips were removed, and a third layer (200 μ l) of 0.5% LMPA was pipetted onto the second layer. The coverslips were then placed back onto the slides and allowed to solidify. The coverslips were removed and the slides submerged in cold lysing solution (500ml; 2.5M NaCl, 100mM EDTA, 1% Triton X-100, 10mM Tris (pH 10) and 10% DMSO) for 1 hour at 4°C. The lysing solution was removed, and the slides were placed into an electrophoresis tank to equilibrate for 20 minutes in alkaline electrophoresis buffer (300mM NaOH and 1mM Na₂EDTA). After equilibration, the tank was sealed, and a current of 300mA (25V) was applied for 35 minutes using a BioRad power supplier. The buffer and slides were carefully removed and the slides were washed three times (5 minutes per wash) with neutralisation buffer (0.4M Tris; pH 7.4).

All slides were then stained with 50 μ l ethidium bromide (20 μ g/ml) and covered with a coverslip. These were then stored overnight at 4°C. The slides were viewed using a fluorescent microscope (Olympus IX5I inverted microscope with 510-560nm excitation and 590nm emission filters) (analySIS Image Processing Software, Novell). Approximately 50 comets per treatment were counted and analysed by measuring tail length (μ m) and by assigning a visual score to each comet based on its appearance according to (Collins, 2004) (Figure 8). The visual score for each treatment was added

up, leaving a score between 0 and 200 arbitrary units for each treatment (50 cells per treatment, with a maximum score of 4 for each cell).

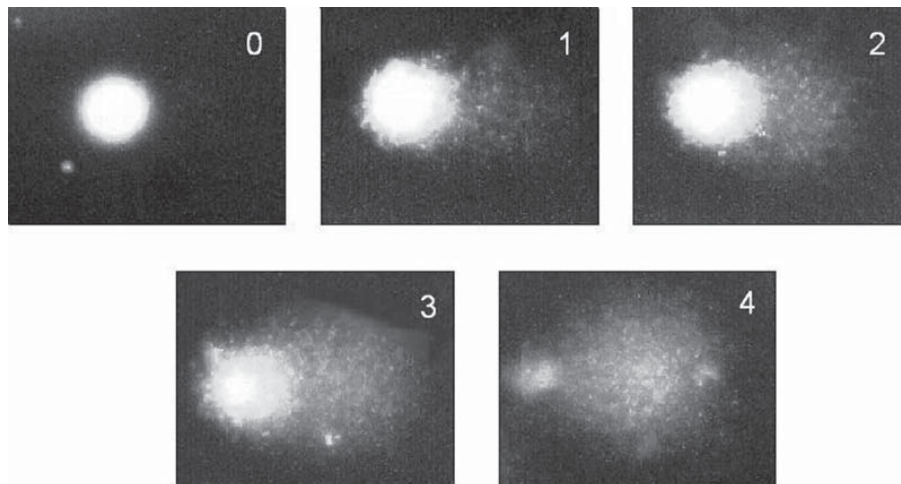


Figure 8: Images used to determine visual scoring of comets following fluorescent microscopy (Collins, 2004).

3.2.9. DNA fragmentation

In order to confirm the results obtained from the SCGE assay, a DNA fragmentation assay was performed. This assay uses gel electrophoresis to show DNA laddering, as well as the presence of DNA strand breaks.

All reagents were prepared according to the protocol in appendix D. Our positive control was prepared using camptothecin (50 μ M), a cytotoxic quinoline alkaloid and S-phase specific anticancer agent that inhibits the DNA enzyme topoisomerase I (topo I) and is implicated in apoptosis, as indicated by among other things chromatin condensation and DNA fragmentation (Lansiaux *et al.*, 2007). A negative control (containing normal DNA from A549 cells (derived from human pulmonary

adenocarcinoma)) was also prepared. Peripheral blood mononuclear cells were not used as a negative control due to time constraints. Treated cells (1×10^6 cells) were centrifuged (Eppendorf centrifuge 5804R, Hamberg, Germany) at 1491rpm for 10 minutes at 24°C. The supernatant was removed and cell lysis solution (600µl) was added to the pellet, which was left to lyse for 15 minutes on ice. Potassium acetate (600µl) was added to the lysed cells, vortexed and mixed by inversion for 8 minutes. The cells were centrifuged (Biofuge Pico, Germany) at 13 000rpm for 5 min, and the remaining supernatant was transferred into a clean Eppendorf tube. Isopropanol (600µl) was added followed by invert mixing for a further 5 minutes. The cells were then centrifuged at 13 000rpm for 5min. The resulting supernatant was removed and placed into a separate Eppendorf. Isopropanol (60µl) was then added to the tube with the supernatant and 200µl to the tube containing the pellet. These were then invert mixed for 5 minutes and centrifuged as above. After centrifuging, the pellets were combined, and 300µl ethanol was added to the final pellet. This was then vortexed and centrifuged as above. The ethanol (supernatant) was removed, and the tubes were inverted and allowed to dry for 15 minutes. Once dry, 40µl of DNA hydration solution (10mM EDTA (pH8, 100mM Tris-cl (pH 7.4) and dH₂O) was added to the pellet. The tubes were then vortexed and placed into a water bath (set to 65°C) for 15 minutes. Once cool, the DNA concentration of each sample was measured using a Nanodrop (Nanodrop 2000). The readings obtained were used to standardise the DNA to the lowest concentration (400ng/µl).

The standardised DNA was electrophoresed after loading samples into 1.8% and 2% gels (Appendix D) containing ethidium bromide (10mg/ml). A voltage of 120V was used, and the gel was then viewed using the UV Tech Alliance 2.7 System (Quantity 1 analysis software).

3.2.10. Annexin V-Fluos

The Annexin V-Fluos assay was performed to detect externalised phosphatidylserine, an early marker of apoptosis, in treated cells (Vermes *et al.*, 1995). Annexin V is a protein that has a high affinity for phosphatidylserine (Koopman *et al.*, 1994). However, since necrotic cells also express phosphatidylserine, a DNA stain (propidium iodide) is used to differentiate between apoptotic and necrotic cells. This resulted in the generation of histograms and scatter plots. The scatter plots present three clusters of cells, including living cells located at the bottom left of the plot, apoptotic cells located at the bottom right of the plot, and necrotic cells located at the top right of the plot.

The protocol was followed according to the manufacturers instructions (BD Biosciences). The samples (1×10^5 cells/ treatment) were transferred to cytometer tubes and then incubated (10 – 15 minutes) in triplicate in 100µl binding buffer containing Annexin-V-FLUOS (diluted in incubation buffer (1ml/10 samples)) and propidium iodide (PI). This was followed by the addition of 0.5ml incubation buffer. The sample data were acquired on a FACSCalibur flow cytometer (BD Biosciences) using the 488 nm excitation and a 515 nm bandpass filter for fluorescein detection and a filter >600 nm for PI detection and then analysed using CellQuest PRO v4.02.

3.2.11. Caspase determination

Activities of initiator caspases 8,9 and effector caspase 3/7 were evaluated using the luminescence-based Promega Caspase-Glo® assay kits, according to manufacturers instructions. This assay is based on the addition of a caspase reagent that results in cell

lysis and caspase cleavage of the substrate (Promega). This generates a luminescent signal that is proportional to the caspase activity present (Promega).

For each measurement, treated cells (1×10^5) were aliquoted into triplicate wells of an opaque luminometer plate. A blank containing cell culture medium only was also prepared.

Briefly, for each assay, 100 μ l of caspase 3/7, 8 or 9 reagent was added to each well that contained the treated cells and mixed using a plate shaker. The plates were then incubated at room temperature for 30 minutes. Following the incubation period, the luminescence of each sample was read on a ModulusTM microplate luminometer (Turner Biosystems, Sunnyvale, USA).

3.2.12. JC - 1 Assay

Flow cytometry was used in order to assess the polarity of the mitochondrial membrane by determining the state of JC-1 (5,5', 6,6'-tetrachloro-1, 1', 3,3'-tetraethylbenzimidazolcarbocyanine iodide), a lipophilic fluorochrome in the cell (BD Biosciences). Once JC-1 enters the cytoplasm, it forms monomers and can be taken up by the mitochondria, where it forms aggregates (BD Biosciences). Red aggregates are measured in the red (FL-2) channel of the flow cytometer, whereas green monomers are measured in the green (FL-1) channel.

Following the manufacturers instructions, treated cells (1×10^6) were prepared in triplicate and 0.5 ml of JC-1 working solution (Appendix E) was added to each sample

pellet. These were then incubated for 15 minutes at 37°C in a CO₂ incubator. Each sample was washed three times with 2ml of JC-1 wash buffer at room temperature. In between each wash step, the cells were centrifuged (centrifuge 5804R, Hamberg, Germany) at 1491rpm for 5 minutes. The samples were resuspended in sheath fluid, and data was acquired using a FACSCalibur bench top cytometer (BD Biosciences) using the 488 nm excitation and a 515 nm bandpass filter for fluorescein. CellQuest PRO v4.02 was used in the analysis of the acquired data. The number of events (15 000) were acquired.

3.2.13. ATP

An ATP assay (Promega) was employed to measure the amount of ATP generated by actively metabolising cells. The principle of this assay is based on the addition of the CellTiter-Glo® Reagent which results in cell lysis and generates a luminescent signal (Promega). This signal is proportional to the amount of ATP, which is directly proportional to the number of cells present (Promega).

For each measurement, 1×10^5 cells/treatment were aliquoted (100µl) into triplicate wells of an opaque luminometer plate. A blank containing cell culture medium only was also prepared. Prior to adding the reagent, an ATP standard curve was prepared according to the manufacturers instructions. The standards were prepared by diluting 1µM ATP (in culture medium) ten times resulting in standards with concentrations ranging from 1µM to 10nM. These were then added (100µl) to the wells of the plate, followed by the addition of 100µl CellTiter-Glo® reagent. The luminescence was then read and the standard curve constructed.

The plate containing the samples was equilibrated at room temperature for 30 minutes. Next, 100µl of CellTiter-Glo® reagent was added to each well and the contents of the plate were then mixed on a plate shaker for 2 minutes to induce cell lysis. This was then incubated for 10 minutes, followed by the detection of luminescence for each sample on a Modulus™ microplate luminometer (Turner Biosystems, Sunnyvale, USA).

3.2.14. Western Blots

Western blot assays are based on the separation of proteins according to molecular weight using sodium dodecyl sulphate polyacrylamide gel electrophoresis (SDS-PAGE) (Osborne & Brooks, 2006). These are then transferred to nitrocellulose membrane and then probed for the binding of various antibodies in order to determine protein expression (Osborne & Brooks, 2006).

Protein was isolated and standardised for use in the western blot assay. All reagents were prepared according to the protocol described in appendix F. The treated cell (1×10^6) pellets were lysed in 200µl of cell lysis buffer (cytobuster (Sigma, Germany) containing 4x protease inhibitor and 4x phosphatase inhibitor) and then placed on ice for 15 minutes. The lysed cells were then centrifuged (Eppendorf 5804R, Hamberg, Germany) at 2 000rpm (4°C) for 10 minutes and the supernatant retained for standardisation and western blotting. Bovine Serum Albumin (BSA) standards (0 – 1mg/ml) were prepared (Appendix F), and 25µl of each (sample and standard) was transferred in duplicate to a 96-well plate. Next, 200µl bicinchoninic acid (BCA) working solution (198µl BCA: 4µl CuSO_4) was added to each well. The absorbance at 562nm was determined using a BioTek MQx200 (South Africa) following an incubation period of 30 minutes at 37°C. After the absorbances were obtained, a standard curve

(Appendix H) was constructed and the proteins standardised to 1mg/ml. Once standardised, 20 μ l of 5x Laemmli sample buffer was added to each sample (100 μ l), which were then denatured at 100°C for 5 minutes. The samples were then stored at -20°C until use.

The denatured samples (25 μ l) and molecular weight marker (5 μ l) were loaded into precast SDS PAGE gels (7.5% resolving and 4% stacking) (Appendix F) and placed in a tank filled with running buffer (Appendix F). Electrophoresis then proceeded at 150V for 1 hour on ice.

Following electrophoresis, the gel was rinsed with deionised water and placed in 1x transfer buffer to equilibrate for 10 minutes. The nitrocellulose membrane and fiber pads were soaked in transfer buffer. Proteins were transferred using the BioRad Trans blot Turbo Transfer system (2.5A, 45 minutes). Briefly, the nitrocellulose membrane was placed onto the fibre pad and the SDS PAGE gel was then placed on top of the membrane, and all air bubbles were removed. Another fibre pad was placed on top of the gel, whilst ensuring no air bubble formation.

After transfer, the membrane was placed into blocking solution (2% BSA) (Appendix F) and then placed on a shaker to block for 1 hour. The blocking solution was discarded and the primary antibody (goat anti - PARP, rabbit anti - NF κ B and mouse anti- heat shock protein (HSP) 70) (1:1000 in 2% BSA) was added to the membrane and allowed to incubate at room temperature for 1 hour with agitation. After the incubation period, the membrane was stored at 4°C overnight.

Next, the membrane was equilibrated on a plate shaker for 1 hour. The primary antibody was removed, and the membrane was washed 3 times with tris-buffered saline and tween 20 (TTBS) (Appendix F) (15 minutes per wash). Following the wash, the secondary antibody dilution (anti-goat IgG for PARP, anti-rabbit IgG for NF κ B and anti Rabbit IgG for HSP 70) (1:1000) was added, followed by an incubation period for 1 hour at room temperature. At the end of the incubation period, the membrane was washed 3 times with TTBS wash buffer as before. The membrane was then rinsed using deionised water and 400 μ l LumiGLO chemiluminescent reagent was added. The membrane was then placed in the UV Tech Alliance 2.7 system (Quantity 1 analysis Software) and the image captured. The same process was performed for β -actin, which was run as a loading control.

3.2.15. Coomassie Blue Staining

For Coomassie staining, the gel was prepared and run as in the western blot. All reagents were prepared according to the protocol described in appendix G. At the end of the run, the gel was stained using 50ml coomassie blue stain for 30min. The stain was then decanted, and the gel was rinsed with 5ml destaining 1 solution (Appendix) (40% Methanol, 10% Acetic acid, 50% dH₂O). It was then incubated on a plate shaker in 100ml destaining solution for 1 hour at room temperature. At the end of the incubation period, destaining 1 was decanted, and the gel was incubated on a shaker for 1 hour in 100ml destaining 2 solution (7% methanol, 10% acetic acid, 83% dH₂O). At the end of the incubation period, destaining 2 solution was decanted and the gel was washed with dH₂O. The stained gel was then scanned and saved.

3.2.16. Data analysis

All data were expressed as mean \pm standard deviation. All statistical analyses were performed on GraphPad Prism version 5 (GraphPad Software, San Diego, California USA). Statistical analyses of the various tests were performed using one-way analysis of variance (ANOVA), with a Bonferroni multiple comparisons test. Values of $p < 0.05$ were considered statistically significant.

CHAPTER 4

RESULTS

4.1. General

The effects of *Tulbaghia violacea* and garlic extracts on Jurkat cells are described in this chapter. The control group consists of untreated cells in CCM.

4.2. MTT Assay

The MTT assay was performed in order to determine the IC₅₀ values for each extract. Figure 9 shows percent cell viability following treatment. All extracts show an increase in % cell viability with increasing extract concentration. However, the % cell viability begins to level off after this increase. These viabilities were used to obtain the IC₅₀ values (Table 1).

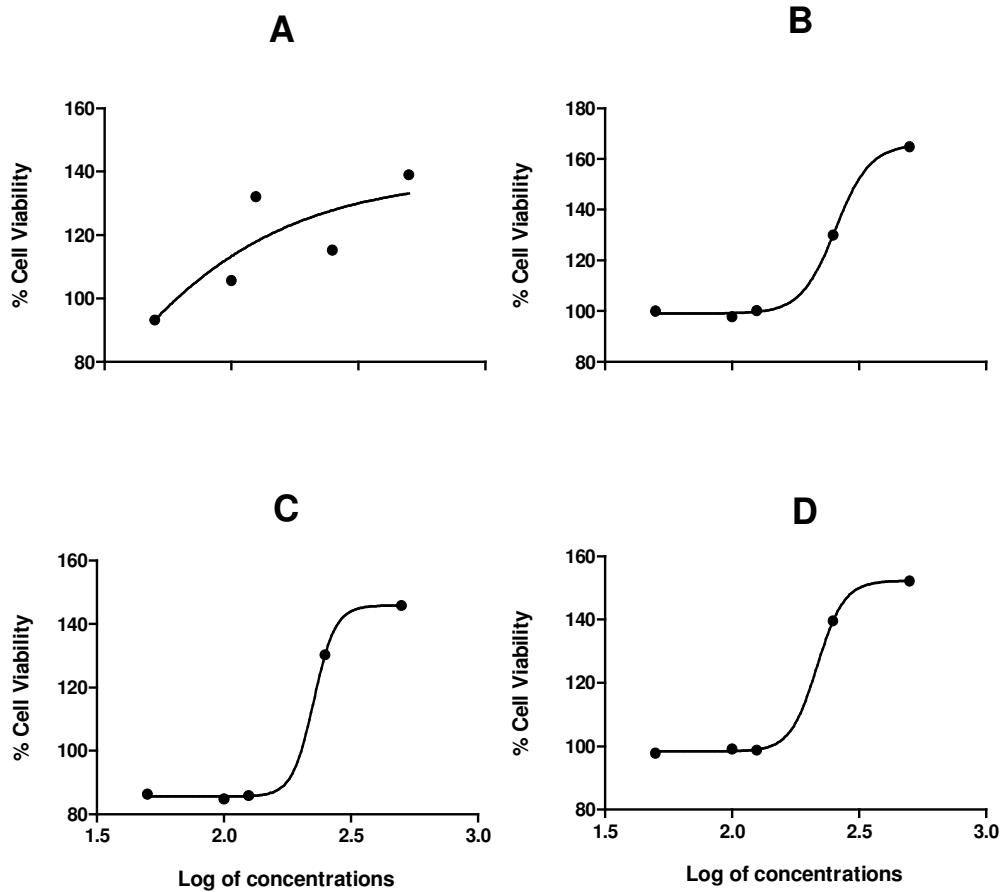


Figure 9: MTT curves showing % cell viability for A) Garlic, B) TV Leaf, C) TV Bulb and D) TV Stalk

Table 1: IC₅₀ values obtained for each extract following an MTT assay

Extracts	IC ₅₀ (µg/ml)
Garlic	14
<i>Tulbaghia violacea</i> leaf	256
<i>Tulbaghia violacea</i> bulb	225
<i>Tulbaghia violacea</i> stalk	216

4.3. TBARS

Lipid peroxidation in the Jurkat cells was measured using the TBARS assay following treatment with various extracts of TV and domesticated garlic (Figure 10). The control MDA concentration of $0.06267 \pm 0.004509 \mu\text{M}$ represents the basal levels of ROS found within the Jurkat cells. All 4 extracts (garlic, TV leaf, TV bulb, TV stalk) exhibited a significant ($p < 0.05$) increase in lipid peroxidation when compared to the control ($0.06267 \pm 0.004509 \mu\text{M}$). Although garlic caused an increase ($p < 0.001$) in MDA concentration (2 fold), the increases observed for the TV extracts were much more pronounced. Of the TV treatments, the bulb ($0.2817 \pm 0.01365 \mu\text{M}$) had the most profound effect, causing a 4.5 fold increase in MDA concentration.

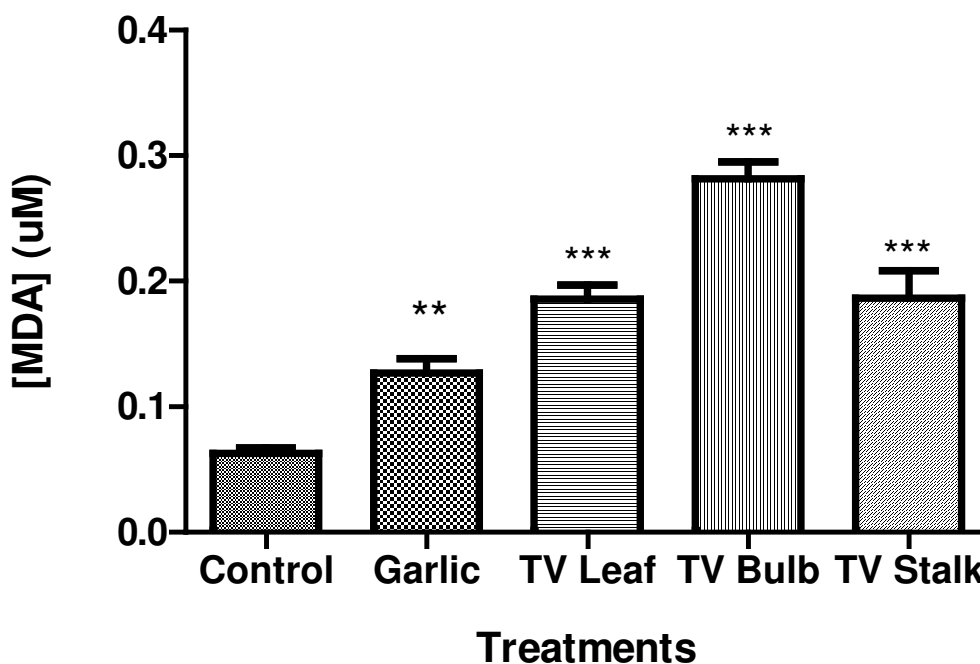


Figure 10: The malondialdehyde (MDA) concentration in Jurkat cells following treatment with garlic and *Tulbaghia violacea* extracts. All treatments caused a dramatic increase in MDA concentration. The samples were run in triplicate, with the assay performed 3 times to validate data. ** $p < 0.001$, and *** $p < 0.0001$ by comparison with the control group.

4.4. Nitric Oxide assay

The NO concentration was determined by extrapolation from a standard curve (Appendix H) following measurement of NO₃ and NO₂, two products of NO breakdown. Figure 11 shows that the only significant increase ($p < 0.001$) in NO concentration was seen in TV bulb and TV stalk. Nitric oxide concentration increased from $3.115 \pm 0.3952 \mu\text{M}$ in the control to $4.787 \pm 0.2116 \mu\text{M}$ in TV bulb, while NO concentration increased from $3.115 \pm 0.3952 \mu\text{M}$ in the control to $4.578 \pm 0.1517 \mu\text{M}$ in TV stalk. However, there was no significant change ($p > 0.05$) in NO concentration for garlic ($2.820 \pm 0.2505 \mu\text{M}$) and TV leaf ($3.447 \pm 0.01927 \mu\text{M}$).

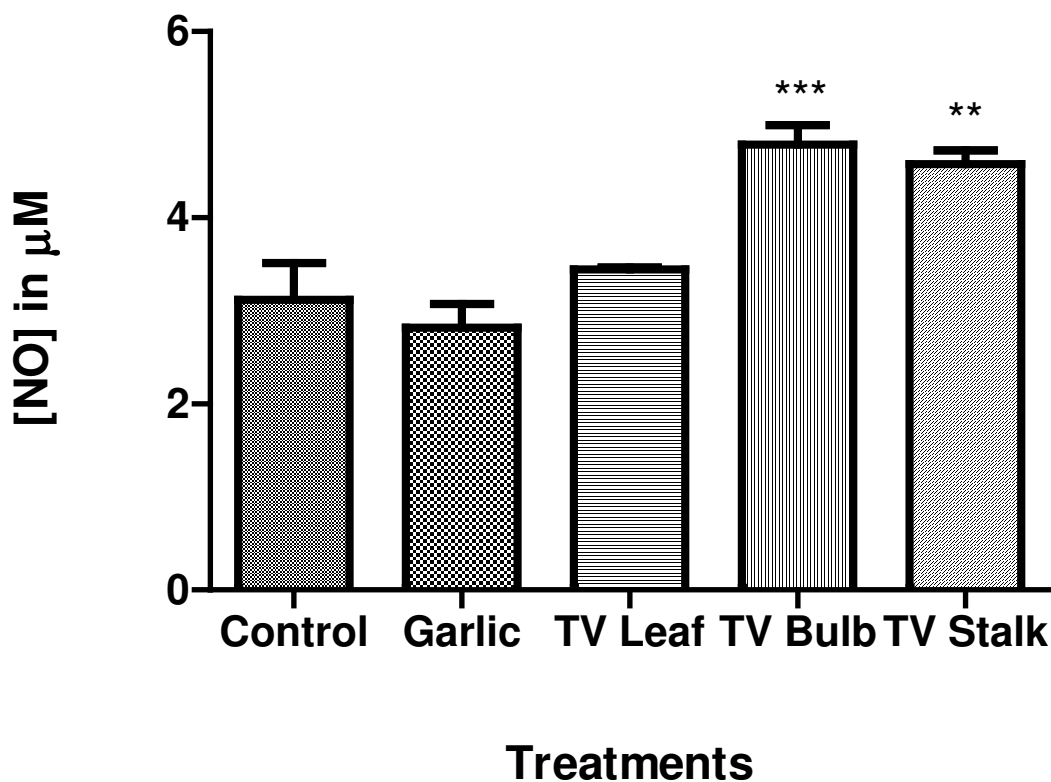


Figure 11: The Nitric Oxide (NO) concentration in Jurkat cells following treatment with garlic and *Tulbaghia violacea* extracts. Only TV bulb and TV stalk treatment resulted in a significant increase in NO concentrations. The assay was performed twice to validate data ** $p < 0.001$, and *** $p < 0.0001$ by comparison with the control group.

4.5. GSH

Luminometry was performed in order to determine the concentration of GSH within the cells (Figure 12). There was a significant ($p < 0.05$) increase in GSH concentrations for TV leaf ($22.93 \pm 0.05136 \mu\text{M}$) and stalk ($22.06 \pm 1.944 \mu\text{M}$) compared to the control ($15.03 \pm 0.3982 \mu\text{M}$). However, there was a non-significant ($p > 0.05$) increase for garlic ($16.73 \pm 1.996 \mu\text{M}$) and TV bulb ($18.17 \pm 0.5145 \mu\text{M}$) respectively.

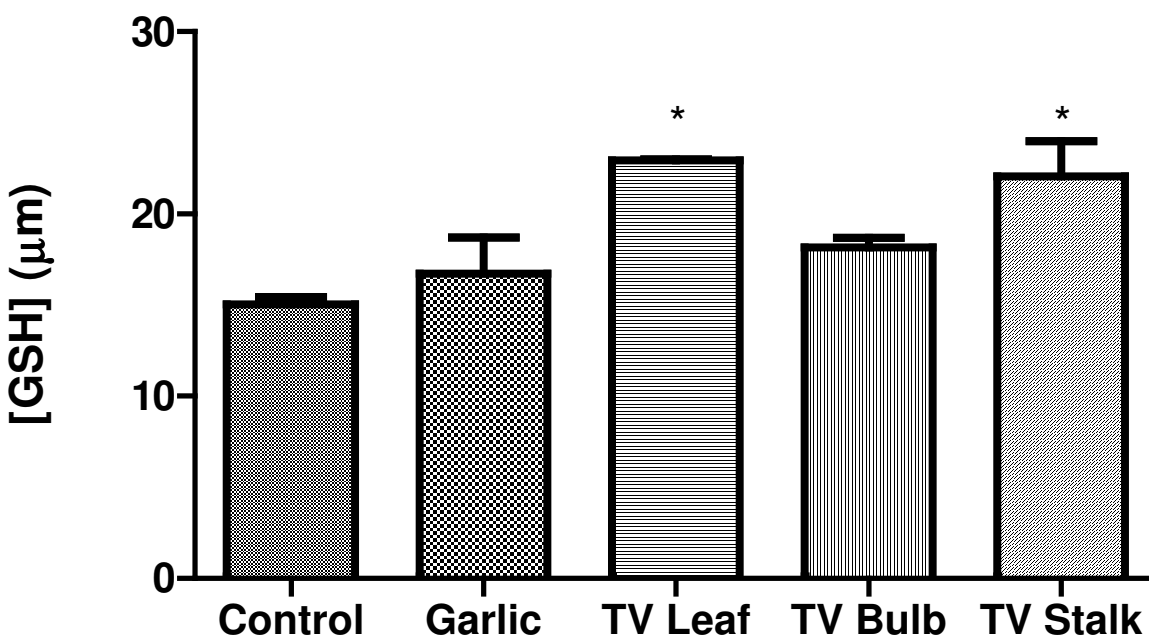


Figure 12: The Glutathione (GSH) **Treatments** concentration in Jurkat cells following treatment with garlic and *Tulbaghia violacea* extracts. Only TV leaf and TV bulb resulted in a significant increase in GSH concentration * $p < 0.05$ by comparison with the control group

4.6. SCGE Assay

To detect the migration of damaged DNA from the nuclear core following electrophoresis, an SCGE assay was performed following exposure to TV and garlic extracts. Representative images from each treatment are shown in Figure 13. Figure 13A represents the control group and shows an intact core in the nucleus. In the treatment groups (13B, 13C, 13D and 13E), the DNA is shown to be migrating out of the nucleus, resulting in comet tail formation. The length of the comet tail (Figure 14) gives an indication of the DNA damage. A significant ($p < 0.05$) increase in comet tail length was seen for all 4 extracts compared to the control, with TV bulb ($21.10 \pm 22.495 \mu\text{m}$) exhibiting the greatest increase in comet tail length (3 fold increase) (Figure 14). Table 2 represents the visual score of the “comets” following treatment. A significant increase in visual score was seen following all treatments. However, the greatest increase was seen following treatment with garlic and in TV bulb. Individual comet visual scores can be seen in Appendix H.

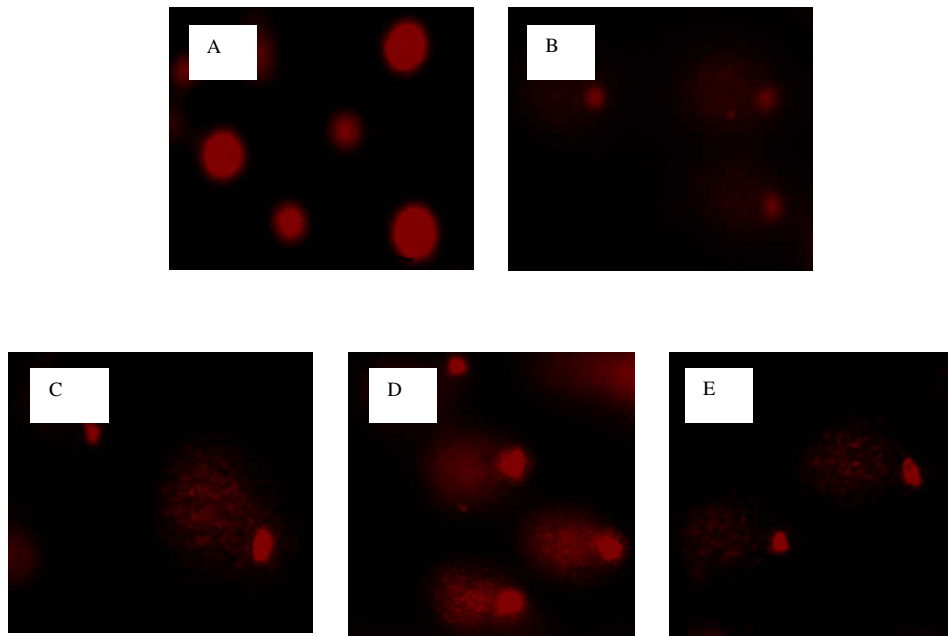


Figure 13: Fluorescent microscope images of Jurkat cells (following treatment with garlic and *Tulbaghia violacea* extracts) showing DNA fragmentation, indicated by the “comet” like appearance of the cells. According to these illustrations, garlic appears to have the most potent effect as seen by the almost total disappearance of the nucleus. A) Control, B) Garlic, C) TV Leaf, D) TV Bulb, and E) TV Stalk (magnification= 400x).

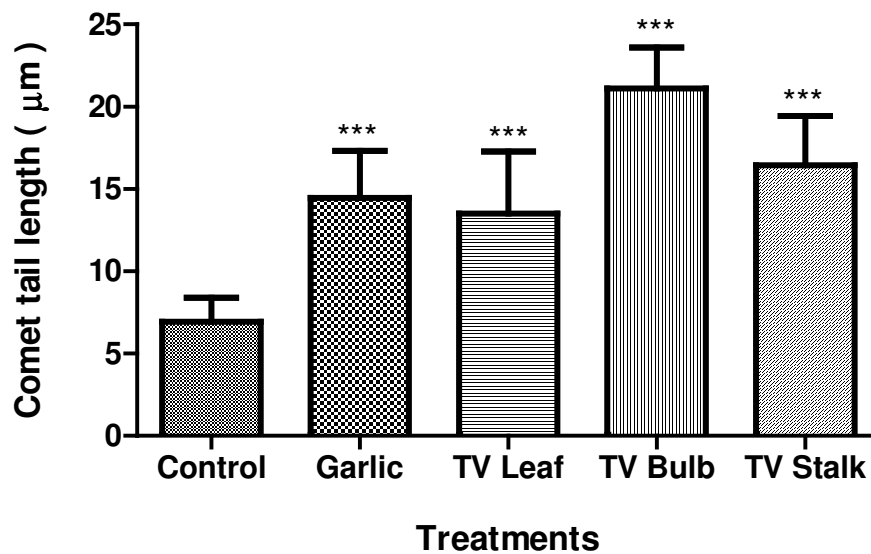


Figure 14: The comet tail length in Jurkat cells following treatment with garlic and *Tulbaghia violacea* extracts. All extracts resulted in an increase in comet tail length, with the greatest increase seen following treatment with TV bulb. *** $p < 0.0001$ by comparison with the control group

Table 2: Visual score of “comets” following treatment with extracts. *** $p < 0.0001$ by comparison with the control group.

Cell numbers	Visual Scores				
	Control	Garlic	TV Leaf	TV Bulb	TV Stalk
1 – 25	5	72	57	80	66
26 - 50	6	68	66	77	71
Total (/200)	11	140***	123***	157***	137***

4.7. DNA Fragmentation

A DNA fragmentation assay was performed in order to detect double or single stranded breaks that may occur following treatments. Figure 15 shows a 1.8% (A) and 2% gel (B). Figure 15A shows single strand (circular form) DNA breaks following treatment with all 4 extracts, with more single strand breaks occurring in TV bulb when compared to the other TV extracts. Figure 15A also shows that double strand (linear form) DNA breaks are occurring in the control and following treatment with garlic extracts. However, double strand breaks appear to be less pronounced in the control when compared to garlic extract. Figure 15B shows the DNA laddering pattern that results due to DNA fragmentation following treatment with the extracts. Laddering is more pronounced in the TV treatments, even though no double strand breaks were observed.

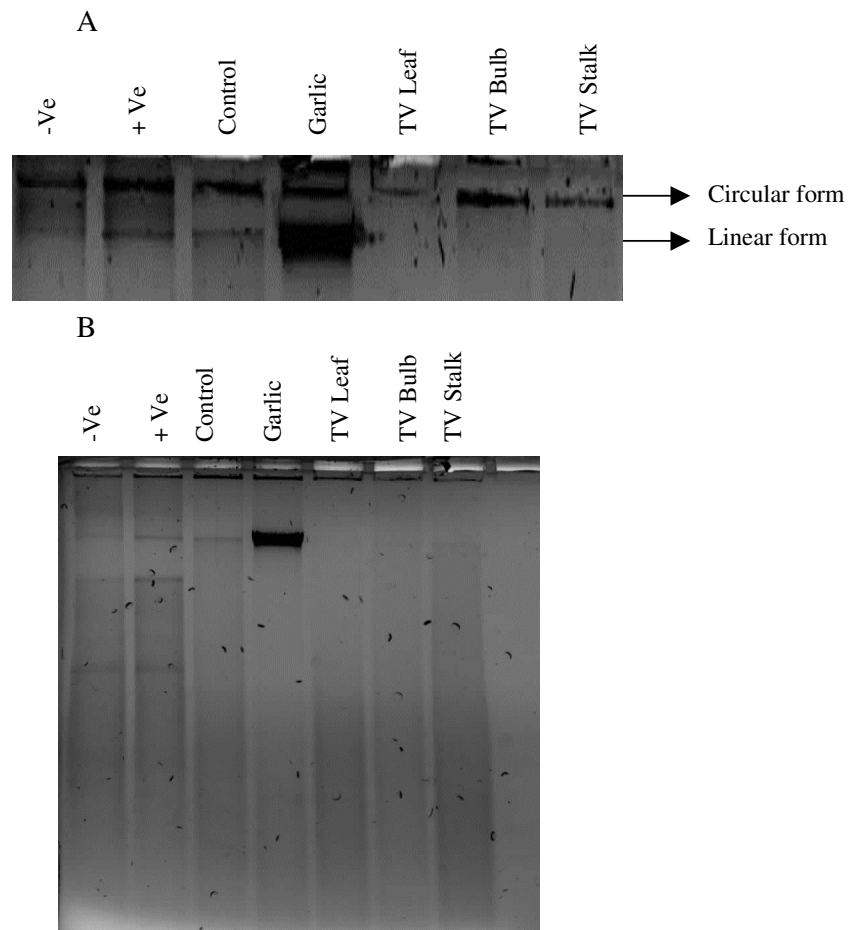


Figure 15: DNA fragmentation in Jurkat cells following treatment with garlic and *Tulbaghia violacea* extracts. A) 1.8% gel, B) 2% gel. The 1.8% gel shows double and single strand breaks, whereas the 2% gel shows laddering DNA fragmentation. The positive control contained 50 μ M camptothecin, whereas the negative control contained normal DNA obtained from A549 cells.

4.8. Annexin V- Fluos

Flow cytometry was performed in order to determine the percentage of living cells (Figure 16A), cells undergoing apoptosis (Figure 16B) and cells undergoing necrosis (Figure 16C) following treatment. No significant difference ($p>0.05$) was found for the percentage of living cells when compared to the control. In figure 16B and C respectively, the control group showed that a low percentage ($5.040\pm 0.04\%$) of cells were undergoing apoptosis, and only $3.330\pm 0.12\%$ of cells were undergoing necrosis.

This suggests that in the control group, the cells were 91.63% viable. Treatment with garlic ($5.620 \pm 0.04\%$), TV bulb ($6.650 \pm 0.02\%$) and TV stalk ($8.210 \pm 0.02\%$) resulted in a significant ($p < 0.0001$) increase in percentage of cells undergoing apoptosis when compared to the control ($5.040 \pm 0.04\%$). *Tulbaghia violacea* stalk extract had the most profound effect, resulting in a 1.6 fold increase ($p < 0.0001$). However, treatment with TV leaf ($4.890 \pm 0.02\%$) resulted in no significant change in percentage of apoptotic cells, instead a slight but non-significant ($p > 0.05$) decrease was observed. Treatment with TV leaf ($4.020 \pm 0.02\%$) resulted in a significant increase ($p < 0.0001$) in percentage cells undergoing necrosis when compared to the control ($3.330 \pm 0.12\%$), whereas TV bulb ($2.640 \pm 0.1\%$) resulted a significant decrease ($p < 0.0001$).

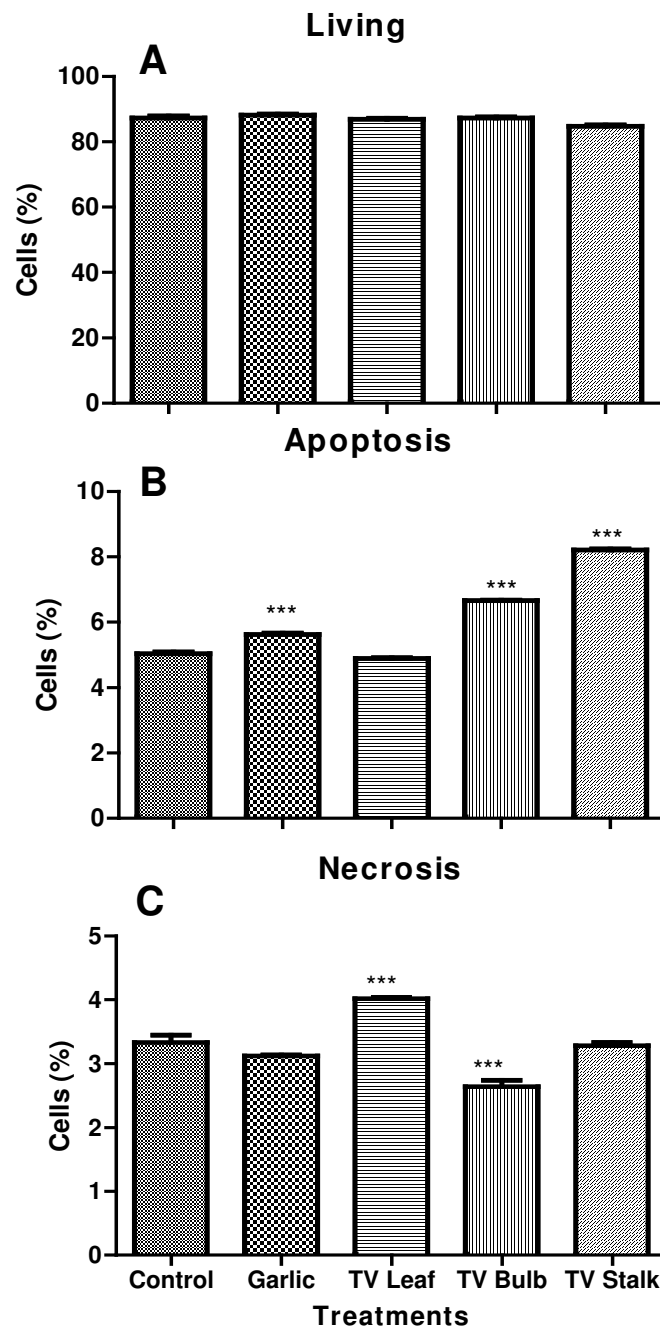


Figure 16: The percentage of living, apoptotic, and necrotic Jurkat cells following treatment with garlic and *Tulbaghia violacea* extracts. A) % Living cells, B) % Cells undergoing apoptosis. All extracts, except TV leaf, resulted in a significant increase in percentage of cells undergoing apoptosis. Treatment with TV leaf induced a significant increase in percentage of cells undergoing necrosis, whereas TV bulb resulted in a significant decrease. *** $p < 0.0001$ by comparison with the control group.

4.9. Caspase activation

Luminometry was performed in order to determine caspase expression in relative light units (RLU). This assay was performed for caspase 3/7 (figure 17A), caspase 8 (figure 17B) and caspase 9 (figure 17C). A significant ($p < 0.05$) increase in the activity of all caspases was observed for TV leaf (caspase 3/7 = 660000 ± 13370 RLU, caspase 8 = 1872000 ± 25120 RLU, caspase 9 = 3750000 ± 41700 RLU). However, treatment with TV bulb extract only resulted in increased caspase 3/7 (58700 ± 62070 RLU) and caspase 9 (3818000 ± 22150 RLU) activity, whereas TV stalk (518700 ± 12830 RLU) resulted in a significant increase only in caspase 3/7 activity. Treatment with the garlic extract resulted in no significant ($p > 0.05$) effects on caspase expression when compared to the control.

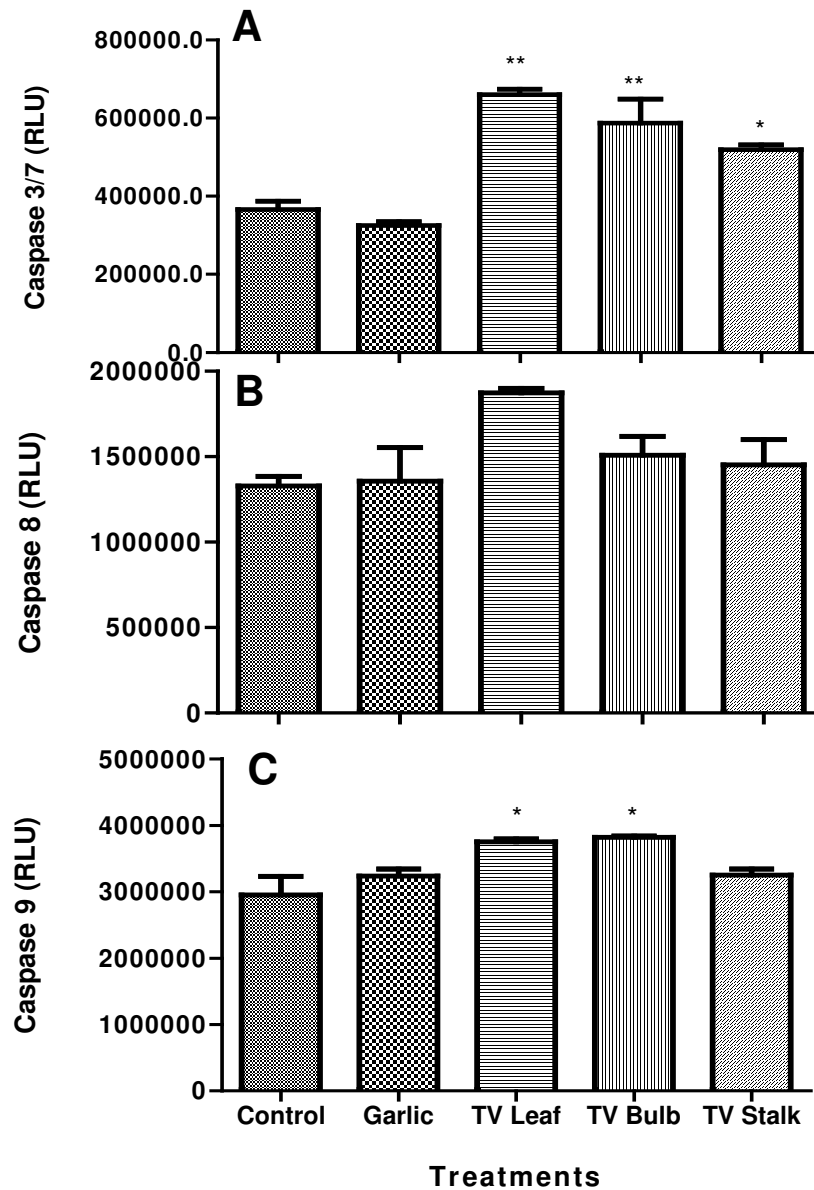


Figure 17: The caspase concentration A) Caspase 3/7, B) Caspase 8, and C) Caspase 9 in Jurkat cells following treatment with garlic and *Tulbaghia violacea* extracts. TV extracts increased caspase 3/7 expression and TV leaf and bulb significantly increased caspase 9 expression. Domesticated garlic had no significant effect on caspase expression. * $p < 0.05$ and ** $p < 0.001$ by comparison with the control group.

4.10. JC-1 Assay

Flow cytometry was performed in order to determine the percentage depolarisation occurring within the cells following treatment (Figure 18). Treatment with TV stalk ($49.2 \pm 0.2\%$) resulted in a significant ($p < 0.05$) increase in percentage depolarisation when compared to the control ($44.10 \pm 0.2\%$). However, treatment with all other extracts resulted in no significant change ($p > 0.05$) in mitochondrial membrane potential.

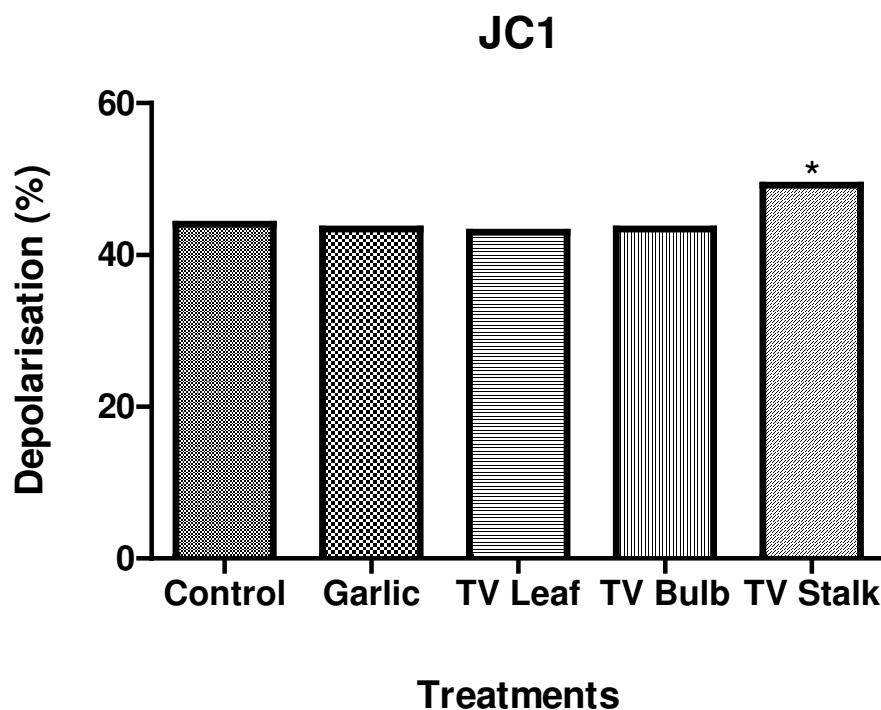


Figure 18: The percentage depolarisation following treatment with garlic and *Tulbaghia violacea* extracts. TV stalk induced a significant increase in percentage depolarisation. All other extracts resulted in no significant change. * $p < 0.05$ by comparison with the control group.

4.11. ATP expression

A CellTiter-Glo® luminescence cell viability assay was performed in order to determine ATP concentration following treatment (Figure 19). No significant changes ($p>0.05$) in ATP concentration were observed, except following treatment with TV leaf (8280000 ± 71080 RLU), which exhibited a significant 1.2 fold increase ($p<0.05$) in ATP concentration compared to the control.

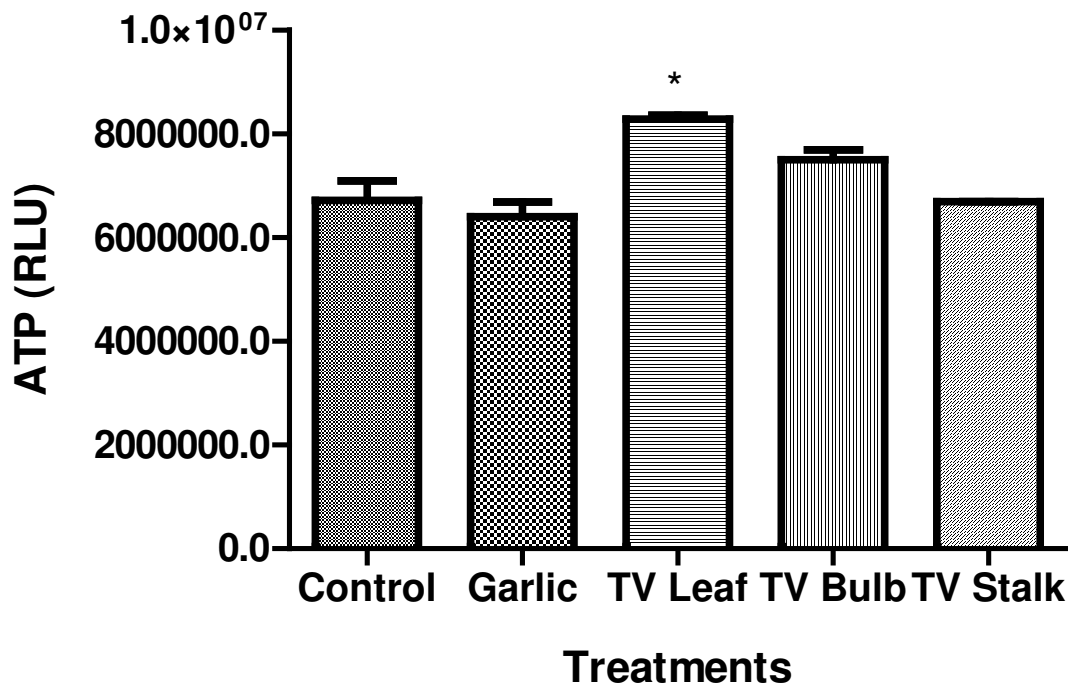


Figure 19: The ATP concentration in Jurkat cells following treatment with garlic and *Tulbaghia violacea* extracts. TV leaf was the only extract to induce a significant increase in ATP concentration. * $p<0.05$ by comparison with the control group

4.12. Coomassie staining

Figure 20 represents the coomassie blue staining of an SDS PAGE gel, and is used to show the presence of total protein, after isolation and extraction.

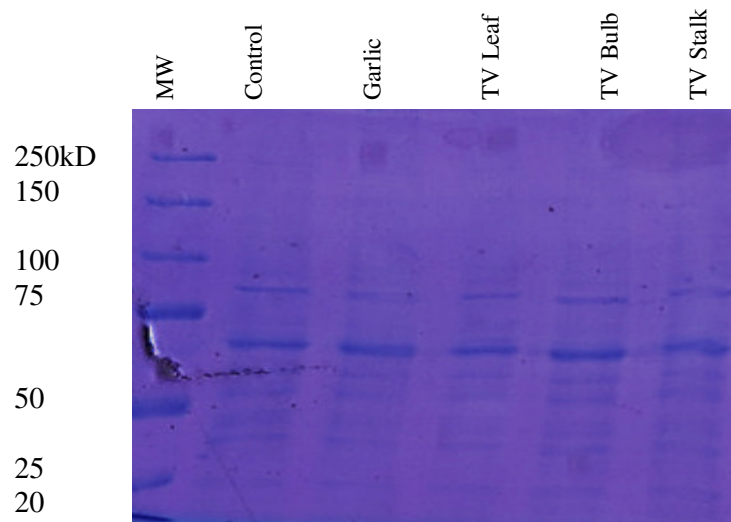


Figure 20: Coomassie Blue stain of SDS PAGE gel following protein extraction

4.13. Western Blots

Western blots were performed in order to determine the expression of a number of proteins (Figure 21). Figure 21A shows the immunoblot obtained using the PARP antibody. This figure shows that PARP cleavage occurred following treatment with all extracts, including the control, with increased expression in TV bulb and stalk. Figure 21B and C show that NF κ B and HSP 70 expression was induced following treatment with all extracts. Expression of NF κ B was greatest following treatment with domesticated garlic.

Figure 21D shows that β - actin is expressed following treatment with all extracts, as well as in the control. This immunoblot was performed as a loading control. Relative band density for each protein is shown in Appendix H.

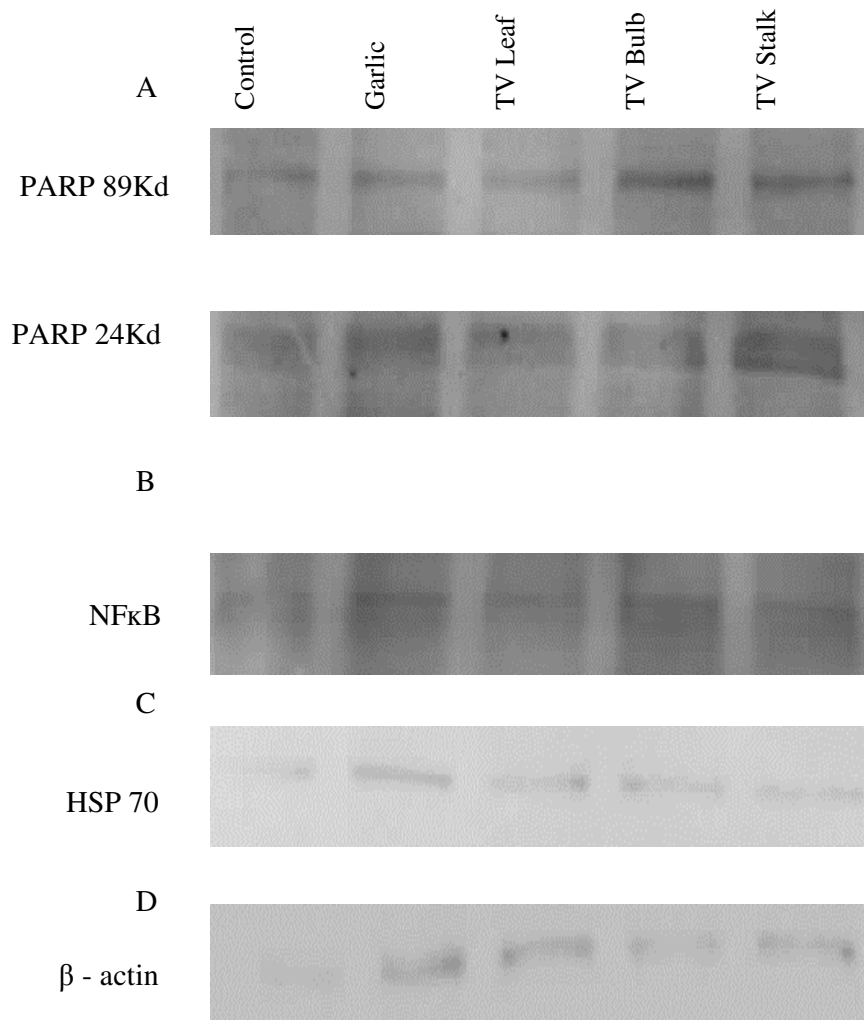


Figure 21: Western blot analyses of apoptotic molecules in Jurkat cells. Isolated proteins were subjected to western blot analyses with the respective antibodies. Cleavage of PARP and expression of NFκB, HSP 70 and β - actin was seen following treatment with all extracts. A) Cleaved PARP bands (89Kd and 24Kd), B) NFκB, C) HSP 70, D) β - actin

Table 3: Summary table showing a summary of all the data for each extract

Assays	Extract			
	TV bulb	TV stalk	TV leaf	Garlic
TBARS	Increase p<0.0001	Increase p<0.0001	Increase p<0.0001	Increase p<0.001
NO	Increase p<0.0001	Increase p<0.001	No change	No change
GSH		Increase p<0.05	Increase p<0.05	No change
Tail length	Increase p<0.0001	Increase p<0.0001	Increase p<0.0001	Increase p<0.0001
Visual scores	Increase p<0.0001	Increase p<0.0001	Increase p<0.0001	Increase p<0.0001
DNA fragmentation	Single strand breaks	Single strand breaks	Single strand breaks	Double strand breaks
% Living	No change	No change	No change	No change
% Apoptosis	Increase p<0.0001	Increase p<0.0001	No change	Increase p<0.0001
% Necrosis	Decrease p<0.0001	No change	Increase p<0.0001	No change
Caspase 3/7	Increase p<0.001	Increase p<0.05	Increase p<0.001	No change
Caspase 8	No change	No change	No change	No change
Caspase 9	Increase p<0.05	No change	Increase p<0.05	No change
% Depolarization	No change	Increase p<0.05	No change	No change
ATP	No change	No change	Increase p<0.05	No change

CHAPTER 5

DISCUSSION

Tulbaghia violacea is a plant indigenous to the Eastern Cape of South Africa that has been used by traditional healers for many years in the treatment of various ailments, including oesophageal cancer (Bungu *et al.*, 2006). However, the mechanisms through which these anti-cancer properties act are not yet known. Studies need to be conducted in order to determine whether or not TV is effective against other types of cancer, as well as oesophageal cancer.

The objective of this study was to determine the effects of *Tulbaghia violacea* and domesticated garlic extracts on Jurkat cells, in an effort to determine whether or not these extracts possess anti-proliferative properties. The results suggest that these extracts do possess apoptosis-inducing properties within Jurkat cells through various mechanisms, including the induction of oxidative stress. The TV extracts were shown to have a greater effect when compared to the domesticated garlic extract. These findings are of great importance, as they present evidence for the possible use of TV as a therapeutic agent for cancer.

The MTT cell viability curves (Figure 9) show that all extracts appear to be increasing percent cell viability. These results are unusual as the results obtained for cells undergoing apoptosis and necrosis indicates that the extracts are inducing cell death. The IC_{50} values calculated from figure 9 represent the half maximal inhibitory concentration. However, as the extracts appear to be increasing cell viability, it would not be possible to calculate these values when there is no inhibition of cell growth. However, it must be noted that the IC_{50} values obtained were in agreement with other

studies (Bungu *et al.*, 2006). The results obtained for the MTT cell viability curves are conflicting, and may be due to human error. However, the experiment was repeated several times with similar results, and can therefore not be explained at this point.

The TBARS assay showed an increase in the concentration of MDA, a by-product of lipid hydroperoxides, in all extracts of TV as well as domesticated garlic (Figure 10). The significant increase in MDA suggests that the extracts are inducing oxidative stress within the Jurkat cells, resulting in lipid peroxidation. This agrees with previous studies which implicated organosulphur compounds (ajoene) found within TV in the induction of ROS in certain cell types, such as promyeloleukemia cells (Kay *et al.*, 2010) (Dirsch *et al.*, 1997). Although this current study did not test the individual compounds within TV, it can be speculated that the increase in ROS may be attributed to the presence of ajoene in the crude extract (Bungu *et al.*, 2006).

This study also demonstrated the difference in potency of the extracts on oxidative stress. The results show that the TV extracts were more potent than domesticated garlic. Of the TV extracts, the bulb induced the greatest increase in MDA concentrations, followed by TV leaf and stalk. Although many studies have tested the effects of TV bulb, this is the first study to test and compare the effects of the three different plant components (bulb, leaf and stalk).

Reactive oxygen species are not the only oxidants produced within cells. Therefore, this study also investigated the production of RNS (NO assay) in response to exposure to TV and garlic extracts. As in the TBARS assay, the TV bulb extract resulted in the greatest significant increase in NO levels (Figure 11). This is the first study that shows a resultant increase in NO levels following treatment with TV bulb. Previous studies have

shown that NO induced apoptosis in Jurkat cells appears to occur via the intrinsic or mitochondrial pathway, as well as activation of the p38/mitogen-activated protein kinase (MAPK) cascade (Ushmorov *et al.*, 1999). This may explain the significant increase seen in percentage of cells undergoing apoptosis for TV bulb (Figure 16B). Previous studies have shown that NO induced apoptosis in Jurkat cells appears to occur via the intrinsic or mitochondrial pathway, as well as activation of the p38/mitogen-activated protein kinase (MAPK) cascade (Ushmorov *et al.*, 1999).

A significant increase in GSH was seen following treatment with TV leaf and stalk, with slight increases ($p > 0.05$) observed following treatment with garlic and TV bulb. This implies that all extracts induced GSH production. However, the increased ROS induced by treatment with TV bulb may result in increased utilisation of GSH, which may account for the minimal change in GSH concentration (Figure 12).

Glutathione acts as a cofactor for glutathione peroxidase (GPx), scavenges ROS directly, buffers NO through formation of a *S*-nitrosoglutathione adduct and is involved in the regulation of various other important antioxidants, such as vitamins C and E (Valko *et al.*, 2007, Wu *et al.*, 2004). Another possible explanation for the GSH results may be attributed to the presence of sulphur containing compounds, which may be higher in the TV stalk and leaf extracts, thus sparing the GSH.

In addition to the lipid peroxidation shown in this study, the ROS and RNS that have been produced also have the ability to exert toxic effects on DNA. All extracts increased DNA damage as shown by the SCGE and DNA fragmentation assays (Figures 14 and 15 respectively). The presence of comet tails indicates the presence of fragmented DNA

that migrates out of the nucleus. The tail lengths and visual scores recorded were the greatest in the bulb (Figure 14 and table 2 respectively). Although the garlic, TV leaf and stalk extracts all increased migration of DNA from the nucleus, this was not as pronounced as that seen in the TV bulb extract.

Studies have shown that initial DNA damage results in cleavage of the supercoiled DNA, producing an “open circular form” (Singh *et al.*, 2009). This represents single strand breaks. Further cleavage results in double strand breaks or “linear double – stranded DNA molecules” (Singh *et al.*, 2009). The DNA fragmentation assay showed high levels of single - strand breaks in the TV bulb extracts (Figure 15A). These results are of significance, as this study is one of the first to show the presence of DNA damage in Jurkat cells following treatment with TV extracts. These results agree with the findings for TBARS and NO production following treatment, as increased ROS and RNS have been known to result in both single and double stranded DNA breaks (Martin, 2008).

Apoptosis can be induced through various mechanisms, including DNA damage (Bohgaki *et al.*, 2010). According to Bohgaki *et al.* (2010), double strand DNA breaks are one of the most serious types of induced DNA damage and can result in cell death. However, natural double stranded DNA breaks (unzipping) also occur that are necessary for normal physiological functions, such as meiosis, the rearrangement of T and B-cell receptors, and during increased gene expression (Bohgaki *et al.*, 2010). This may explain the results seen for the control group (Figure 15A). Both single and double strand DNA breaks have been found to activate p53, a tumour suppressor that plays a role in the regulation of apoptosis (Bohgaki *et al.*, 2010, Nelson & Kastan, 1994).

Although the SCGE and DNA fragmentation assays alone cannot be used to detect apoptosis, they have been used to verify and support all other results (Collins, 2004).

The Annexin V-Fluos assay detects externalised phosphatidylserine as a marker of apoptosis. Phosphatidylserine has been shown to become translocated to the outer layer of the plasma membrane during the early stages of apoptosis (Vermes *et al.*, 1995). This translocation allows phagocytes such as macrophages to identify the apoptotic cell and facilitate its removal (Fadok *et al.*, 1992). This assay showed that the garlic, TV bulb and TV stalk extracts induced a significant increase in the percentage of cells undergoing apoptosis, with the most significant increase observed for TV stalk (Figure 16B). This agrees with the findings of Bungu *et al.* who showed that TV bulb extracts induced apoptosis within cancer cell lines such as the MCF-7, WHCO3, HT29 and HeLa cell lines (Bungu *et al.*, 2006). However, this is the first study to show the induction of apoptosis by TV stalk extracts in a Jurkat cell line. Although the extracts did appear to induce an increase in the percentage of cells undergoing apoptosis, this increase was not to a great extent. This may be explained by the occurrence of natural physiological apoptosis. However, further studies need to be conducted to differentiate between natural and induced apoptosis.

The increased ROS, RNS and DNA damage occur in conjunction with this increase in percentage of cells undergoing apoptosis (Figure 16B). It can therefore be hypothesised that one way by which TV induces apoptosis within Jurkat cells, is the induction of oxidative stress. This link between oxidative stress and apoptosis has been shown previously (Kannan & Jain, 2000). The induction of apoptosis through oxidative stress has been attributed to an organosulphur compound (ajoene) found within TV (Dirsch *et*

al., 1997, Kay *et al.*, 2010). In order to determine which apoptotic pathway is activated, caspase activity was determined (Figure 17).

Apoptosis can occur through the extrinsic pathway, intrinsic pathway, or both (Tang *et al.*, 2008). Various enzymes, including caspases, are involved in the regulation of these pathways (Cohen, 1997). During the intrinsic pathway, cytochrome C is released from the mitochondria where it complexes with apoptotic protease activating factor (apaf)-1 and pro-caspase 9 resulting in apoptosome formation and leads to the activation of caspase 9 (Jiang & Wang, 2004). Activated caspase 9 then activates caspase 3/7, which effects the process of apoptosis (Jiang & Wang, 2004). The extrinsic pathway is triggered by the Fas death receptor and TNF and results in the activation of pro-caspase 8, and eventually caspase 3 (Tang *et al.*, 2008).

The activation of caspase 9 and caspase 3/7 (Figure 17) by TV extracts suggests that apoptosis is proceeding through the intrinsic pathway. Activated caspase 3/7 is responsible for the cleavage of PARP during the execution phase of apoptosis (Cohen, 1997). Cleavage of PARP results in increased utilisation of ATP for apoptosis, and also interferes with its normal function as a DNA repair enzyme (Cohen, 1997).

Tulbaghia violacea stalk showed a significant increase in mitochondrial depolarisation (Figure 18), which correlates with the induction of apoptosis (figure 16B) and caspase 3/7 activation (Figure 17A). Studies have implicated mitochondrial depolarisation in the release of cytochrome C and the induction of apoptosis (Gao *et al.*, 2001, Heiskanen *et al.*, 1999). One hypothesis suggests that a channel (permeability transition pore) in the inner mitochondrial membrane is induced to open during apoptosis resulting in the

rupture of its outer membrane and the subsequent release of cytochrome C (Gao *et al.*, 2001). Increased mitochondrial depolarisation confirms the hypothesis that suggests that TV stalk may act through the intrinsic apoptotic pathway. Studies have shown that mitochondrial dysfunction appears to occur prior to cell shrinkage and nuclear fragmentation when apoptosis is taking place (Kroemer *et al.*, 2007).

The domesticated garlic extract resulted in no significant change in caspase 3/7 or 9 activation (Figures 17A and C respectively), even though percentage of cells undergoing apoptosis was increased. This suggests that domesticated garlic may induce caspase-independent apoptosis. The domesticated garlic extract may also contain highly efficient apoptosis-inducing properties. Also, due to the rapid rate of degradation of caspases once they have performed their function, the increased activity that was expected may not be seen following treatment with this extract. However, further studies need to be undertaken in order to confirm these hypotheses.

Tulbaghia violacea leaf was the only extract that did not show a significant change in the percentage of cells undergoing apoptosis (figure 16B). However, it was the only extract that resulted in a significant increase in percentage cells undergoing necrosis (figure 16C). However, this increase was not to a great extent. These results are specific to treatment with the TV leaf extract and are unusual as caspase 3/7 and 9 expression increased significantly following treatment with all extracts, including TV leaf (Figures 17A and C respectively).

A possible explanation for this occurrence is the development of secondary necrosis within the Jurkat cells following treatment. Secondary necrosis is defined as “an

autolytic process of cell disintegration with release of cell components that occurs when there is no intervention of scavengers and the full apoptotic programme is completed” (Silva, 2010). This process is different to primary necrosis, as it occurs after apoptosis and results in the release of activated caspase 3 (Figure 17A) (Silva, 2010).

However, the hypothesis of secondary necrosis is contradictory to the results shown in Figure 19. This figure shows a significant increase in ATP production following treatment with TV leaf, with no change in ATP production following treatment with all other extracts. Studies have shown that secondary necrosis results in a decrease in ATP production, as a result of increased consumption of NAD and decreased glucose breakdown (Zong & Thompson, 2006). This increased NAD consumption has been shown to be due to acute PARP activation which occurs as a result of DNA strand breaks (Zong & Thompson, 2006).

Another possible explanation for induction of necrosis by TV leaf may be the hyperactivation of PARP. In some cases, PARP can become hyperactivated resulting in necrosis (Zong & Thompson, 2006). However, further studies need to be conducted in order to confirm this hypothesis. Figure 21A shows that treatment with TV and domesticated garlic extracts results in PARP cleavage, confirming that apoptosis is taking place. As mentioned previously, this cleavage is due to the activation of caspase 3/7 (Bungu *et al.*, 2006).

Figure 21B shows that NFκB is being expressed following treatment with all 4 extracts, suggesting that it may play a role in the initiation of apoptosis. Pro-apoptotic NFκB

activated during oxidative stress following the activation of p38/mitogen-activated protein kinase (MAPK) cascades (Cen & Packer, 1996).

According to Golli-Bennour and Bacha, HSP70 is an important regulatory protein that is expressed during stressful conditions (Golli-Bennour & Bacha, 2011). Even though there is increased stress, the HSP 70 is not being differentially expressed in this study (Figure 21C and Appendix H). This suggests that these cancer cells present with an aberrant stress response. An aberrant stress response has been found in previous cancer studies, including a study conducted on prostate cancer that found aberrant expression of activating transcription factor 3 (ATF3) (Wang *et al.*, 2012).

One function of HSP70 is to block or inhibit apoptosis through the inhibition of apoptosis inducing factor (AIF) and Apaf-1, thereby protecting the cell (Golli-Bennour & Bacha, 2011). As a result, failure to up-regulate HSP70 may result in apoptotic cell death as reported in this study. However, the results presented for the western blot data still need to be verified.

CHAPTER 6

CONCLUSION

This study showed that *T. violacea* and garlic extracts have the potential to induce oxidative stress in the form of either ROS or RNS within the Jurkat cells. The resultant oxidative stress predisposes the cells to DNA damage and eventually apoptosis, with the most significant effects observed following treatment with the *T. violacea* extracts.

More importantly, this is the first study to compare the potency of the different plant components. It is also the first to show a resultant increase in NO levels following treatment with TV bulb, as well as the presence of DNA damage in Jurkat cells following treatment with TV extracts. Previous studies have highlighted the effects of TV bulb and leaf; however, this is the first to investigate the effects of *Tulbaghia violacea* stalk extracts on Jurkat cells and show that these extracts are inducing apoptosis within this cell line. The results shown in this study may be of clinical significance, as cell death through apoptosis is the preferred method of action for anti-cancer drugs. However, further studies need to be conducted, as the MTT data showed an increase in cell viability following treatment. This conflicts with the results obtained for the Annexin V-Fluos. However, the apoptosis results also revealed only a slight increase in cells undergoing apoptosis.

The present study had a few limitations, in that crude extracts were used. Therefore, other factors may be present that affected the results. Also, the suggested reasons for the observed increase in the percentage of cells undergoing necrosis following treatment with TV leaf could not be verified. In order to determine whether or not secondary necrosis is occurring, further studies need to be performed. The mechanism by which

the extracts induced GSH activity are still unknown and are therefore subject to further investigation. The activities of the other antioxidants (SOD, catalase and GPx) were not measured, and therefore could not be compared to the GSH results.

Although Jurkat cells have been found to be very useful, they contain several abnormalities. This cell line has previously been shown to be deficient in several lipid phosphatases (Abraham & Weiss, 2004). These include PTEN (Phosphatase and Tension homologue) and SHIP (SH2 - domain - containing inositol polyphosphate 5' phosphatase) (Abraham & Weiss, 2004). These phosphatases act to regulate the phosphoinositide- 3- kinase (PI3K) pathway (Abraham & Weiss, 2004). As a result, deficiency of PTEN and SHIP can lead to increased expression of protein kinase B (AKT), increased levels of phosphorylated phosphoinositide lipids, and association of IL2-inducible T-cell kinase (Itk) with the Jurkat cell plasma membrane (Bartelt *et al.*, 2009).

Although this study shows that *T. violacea* appears to be cytotoxic to Jurkat cells, its effects on healthy peripheral blood mononuclear Cells (PBMCs) are not yet known. This is a vital part of the study, as these results would constitute a normal control. Molecular studies also need to be conducted in order to determine and isolate the exact compounds responsible for the cytotoxic activity. Also, other components of the plant (flower) still need be studied for possible anti-proliferative effects. It may also be useful to repeat the study using other T cell leukaemic cell lines (such as CCRF-CEM-VLB100) for comparison, as well as PBMCs.

REFERENCES

- Abraham, R. T., and Weiss, A. (2004) Jurkat T cells and development of the T-cell receptor signalling paradigm, *Nature* 4, 301-308.
- Aggarwala, B. B., Shishodia, S., Sandur, S. K., Pandey, M. K., and Sethi, G. (2006) Inflammation and cancer: How hot is the link?, *Biochemical Pharmacology* 72, 1605-1621.
- Alscher, R. G., Erturk, N., and Heath, L. S. (2002) Role of Superoxide Dismutases (SODs) in Controlling Oxidative Stress in Plants, *Journal of Experimental Botany* 53, 1331-1341.
- Amagase, H. (2006) Significance of Garlic and Its Constituents in Cancer and Cardiovascular Disease, *Journal of nutrition* 136, 716S–725S.
- Aust, A. E., and Eveleigh, J. F. (1999) Mechanisms of DNA Oxidation, *Proceedings of the Society for Experimental Biology and Medicine* 222, 246-252.
- Auyang, S. Y. (2004) Cancer causes and cancer research on many levels of complexity, *Creating Technology*, 1-15.
- Aviello, G., Abenavoli, L., Borrelli, F., Capasso, R., Izzo, A. A., Lembo, F., Romano, B., and Capasso, F. (2009) Garlic: Empiricism or Science?, *Natural Product Communications* 4, 1785-1796.
- Bartelt, R. R., Cruz-Orcutt, N., Collins, M., and Houtman, J. C. D. (2009) Comparison of T Cell Receptor-Induced Proximal Signaling and Downstream Functions in Immortalized and Primary T Cells, *PLoS ONE* 4, 1-16.

- Bennett, M. R. (2001) Reactive Oxygen Species and Death Oxidative DNA Damage in Atherosclerosis, *Circulation Research* 88, 648-650.
- Bohgaki, T., Bohgaki, M., and Hakem, R. (2010) DNA double-strand break signaling and human disorders, *Genome Integrity* 1, 1-14.
- Brown, J. M., and Attardi, L. D. (2005) The role of apoptosis in cancer development and treatment response, *Nature* 5, 231-237.
- Bungu, L., Frost, C. L., Brauns, S. C., and Van De Venter, M. (2006) Tulbaghia violacea inhibits growth and induces apoptosis in cancer cells in vitro, *African Journal of Biotechnology* 5, 1936-1943.
- Bungu, L., Van De Venter, M., and Frost, C. (2008) Evidence for an in vitro anticoagulant and antithrombotic activity in Tulbaghia violacea, *African Journal of Biotechnology* 7, 681-688.
- Burton, G. W., and Traber, M. G. (1990) Vitamin E: Antioxidant Activity, Biokinetics, and Bioavailability, *Annual Review of Nutrition* 10, 357-382.
- Cao, C., Leng, Y., and Kufe, D. (2003) Catalase Activity Is Regulated by c-Abl and Arg in the Oxidative Stress Response, *The Journal of Biological Chemistry* 278, 29667-29675.
- Carr, A., and Frei, B. (1999) Does vitamin C act as a pro-oxidant under physiological conditions?, *The Journal of The Federation of American Societies for Experimental Biology* 13, 1007-1024.
- Cassileth, B. R. (1999) Evaluating Complementary and Alternative Therapies for Cancer Patients, *Cancer Journal For Clinicians* 49, 362-375.

- Catalá, A. (2009) Lipid peroxidation of membrane phospholipids generates hydroxy-alkenals and oxidized phospholipids active in physiological and/or pathological conditions, *Chemistry and Physics of lipids* 157, 1-11.
- Cen, C. K., and Packer, L. (1996) Antioxidant and redox regulation of gene transcription, *Federation of American Societies for Experimental Biology Journal* 10, 709-720.
- Center, M., Siegel, R., and Jema, A. (2011) Global Cancer Facts & Figures 2nd Edition, *Atlanta: American Cancer Society*.
- Cohen, G. M. (1997) Caspases: the executioners of apoptosis, *Biochemical Journal* 326, 1-16.
- Collins, A. R. (2004) The Comet Assay for DNA Damage and Repair, *Molecular Biotechnology* 26, 249-261.
- Devasagayam, T. P. A., Tilak, J. C., Bloor, K. K., Sane, K. S., Ghaskadbi, S. S., and Lele, R. D. (2004) Free Radicals and Antioxidants in Human Health: Current Status and Future Prospects, *Journal of the Association of Physicians of India* 52, 794-804.
- Dirsch, V. M., Gerbes, A. L., and Vollmar, A. M. (1997) Ajoene, a Compound of Garlic, Induces Apoptosis in Human Promyeloleukemic Cells, Accompanied by Generation of Reactive Oxygen Species and Activation of Nuclear Factor kB, *Molecular Pharmacology* 53, 402-407.

- Dorant, E., Van Den Brandt, P. A., Goldbohm, R. A., Hermus, R. J. J., and Sturmans, F. (1993) Garlic and its significance for the prevention of cancer in humans: a critical view, *British Journal of Cancer* 67, 424-429.
- Fadok, V. A., Voelker, D. R., Campbell, P. A., Cohen, J. J., Bratton, D. L., and Henson, P. M. (1992) Exposure of phosphatidylserine on the surface of apoptotic lymphocytes triggers specific recognition and removal by macrophages, *The Journal of Immunology* 148, 2207-2216.
- Fang, Y., Yang, S., and Wu, G. (2002) Free Radicals, Antioxidants, and Nutrition, *Nutrition* 18, 872– 879.
- Farmer, J. D., and Packard, N. H. (1986) The immune system, adaptation, and machine learning, *Physica* 22, 187-204.
- Fiaschi, T., and Chiarugi, P. (2012) Oxidative Stress, TumorMicroenvironment, and Metabolic Reprogramming: A Diabolic Liaison, *International Journal of Cell Biology* 2012, 1-8.
- Fidan, A. F., Kucukkurt, I., Yuksel, H., Ozdemir, A., Ince, S., and Dundar, Y. (2009) The Effects of Structurally Different Saponin Containing Plants on Tissue Antioxidant Defense Systems, Lipid Peroxidation and Histopathological Changes in Streptozotocin-Induced Diabetic Rats, *Journal of Animal and Veterinary Advances* 8, 920-927.
- Gao, W., Pu, Y., Luo, K. Q., and Chang, D. C. (2001) Temporal relationship between cytochrome c release and mitochondrial swelling during UV-induced apoptosis in living HeLa cells, *Journal of Cell Science* 114, 2855-2862

- Golli-Bennour, E. E., and Bacha, H. (2011) Hsp70 expression as biomarkers of oxidative stress: Mycotoxins' exploration, *Toxicology* 287, 1-7.
- Gongora, M. C., Qin, Z., Laude, K., Kim, H. W., McCann, L., Folz, J. R., Dikalov, S., Fukai, T., and Harrison, D. G. (2006) Role of Extracellular Superoxide Dismutase in Hypertension, *Hypertension* 48, 473-481.
- Gribbni, M. A., Hardisty, R. M., Chessells, J. M. (1977) Long-term control of central nervous system leukaemia, *Archives of Disease in Childhood* 52, 673-678.
- Grivennikov, S. I., Greten, F. R., and Karin, M. (2010) Immunity, Inflammation, and Cancer, *Cell* 140, 883-899.
- Halliwell, B. (2006) Reactive Species and Antioxidants. Redox Biology Is a Fundamental Theme of Aerobic Life , *Plant Physiology* 141, 312–322.
- Heiskanen, K. M., Bhat, M. B., Wang, H., Ma, J., and Nieminen, A. (1999) Mitochondrial Depolarization Accompanies Cytochrome cRelease During Apoptosis in PC6 Cells, *The Journal of Biological Chemistry* 274, 5654-5658.
- Jiang, X., and Wang, X. (2004) Cytochrome C - Mediated Apoptosis, *Annual Review of Biochemistry* 73, 87–106.
- Kannan, K., and Jain, S. K. (2000) Oxidative stress and apoptosis, *Pathophysiology* 7, 153–163.
- Kay, H. Y., Yang, J. W., Kim, T. H., Lee, D. Y., Kang, B., Ryu, J., Jeon, R., and Kim, S. G. (2010) Ajoene, a Stable Garlic By-Product, Has an Antioxidant Effect through Nrf2-Mediated Glutamate-Cysteine Ligase Induction in HepG2 Cells and Primary Hepatocytes, *The Journal of Nutrition* 140, 1211-1219.

- Kidd, P. M. (1997) Glutathione: Systemic Protectant Against Oxidative and Free Radical Damage, *Alternative Medicine Review* 2, 155-176.
- Koopman, G., Reutelingsperger, C. P., Kuijten, G. A., Keehnen, R. M., Pals, S. T., and van Oers, M. H. (1994) Annexin V for flow cytometric detection of phosphatidylserine expression on B cells undergoing apoptosis, *84*, 1415-1420.
- Kroemer, G., Galluzzi, L., and Brenner, C. (2007) Mitochondrial Membrane Permeabilization in Cell Death, *Physiological Reviews* 87, 99-163.
- Lansiaux, A., Leonce, S., Kraus-Berthier, L., Bal-Mahieu, C., Mazinghien, R., Didier, S., David-Cordonnier, M. H., Hautefaye, P., Lavielle, G., Bailly, C., Hickman, J. A., and Pierre, A. (2007) Novel stable camptothecin derivatives replacing the E-ring lactone by a ketone function are potent inhibitors of topoisomerase I and promising antitumor drugs, *Mol Pharmacol* 72, 311-319.
- Lyantagaye, S. L. (2011) Ethnopharmacological and Phytochemical review of allium species (sweet garlic) and Tulbaghia species (wild garlic) from Southern Africa, *Tanzania Journal of Science* 37, 58-72.
- Marnett, L. J. (2002) Oxy radicals, lipid peroxidation and DNA damage, *Toxicology* 181, 219-222.
- Martin, L. J. (2008) DNA Damage and Repair: Relevance to Mechanisms of Neurodegeneration, *J Neuropathol Exp Neurol* 67, 377-387.
- Martínez, M. C., and Andriantsitohaina, R. (2009) Reactive Nitrogen Species: Molecular Mechanisms and Potential Significance in Health and Disease, *Antioxidants & Redox Signaling* 11, 669-702.

- Matsura, T., Kai, M., Fujii, Y., Ito, H., and Yamada, K. (1999) Hydrogen peroxide-induced apoptosis in HL-60 cells requires caspase-3 activation, *Free Radical Research* 30, 73-83.
- Molassiotis, A., Fernandez-Ortega, P., Pud, D., Ozden, G., Scott, J. A., Panteli, V., Margulies, A., Browall, M., Magri, M., Selvekerova, S., Madsen, E., Milovics, L., Bruyns, I., Gudmundsdottir, G., Hummerston, S., Ahmad, A. M. A., Platin, N., Kearney, N., and Patiraki, E. (2005) Use of complementary and alternative medicine in cancer patients: a European survey, *Annals of Oncology* 16, 655-663.
- Mosmann, T. (1983) Rapid Colorimetric Assay for Cellular Growth and Survival: Application to Proliferation and Cytotoxicity Assays *Journal of Immunological Methods* 65, 55-63.
- Murphy, N., Shultz, J., Zhou, W., and Woo, K. V. (2008) Detecting Toxicological Responses in Cells with the Bioluminescent GSH-GLO™ Glutathione Assay, *Cell Notes*.
- Nash, K. M., Rockenbauer, A., and Villamena, F. A. (2012) Reactive Nitrogen Species Reactivities with Nitrones: Theoretical and Experimental Studies, 25 8, 1581–1597.
- Neher, D. A., and Stürzenbaum, S. R. (2006) Extra-long PCR, an identifier of DNA adducts in single nematodes (*Caenorhabditis elegans*), *Comparative Biochemistry and Physiology* 144, 279–285.

- Nelson, W. G., and Kastan, M. B. (1994) DNA Strand Breaks: the DNA Template Alterations That Trigger p53-Dependent DNA Damage Response Pathways, *Molecular and Cellular Biology* 14, 1815-1823.
- Nordberg, J., and Arner, E. S. J. (2001) Reactive Oxygen Species, Antioxidants, and the Mammalian Thioredoxin System, *Free Radical Biology & Medicine* 13, 1287–1312.
- Olorunnisola, O. S., Bradley, G., and Afolayan, A. J. (2012) Effect of methanolic extract of *Tulbaghia violacea* rhizomes on antioxidant enzymes and lipid profile in normal rats., *African Journal of Pharmacy and Pharmacology* 6, 1026 - 1030.
- Oommen, S., Anto, R. J., Srinivas, G., and Karunagaran, D. (2004) Allicin (from garlic) induces caspase-mediated apoptosis in cancer cells, *European Journal of Pharmacology* 485, 97-103.
- Osborne, C., and Brooks, S. A. (2006) SDS-PAGE and Western blotting to detect proteins and glycoproteins of interest in breast cancer research., *Methods in Molecular Medicine* 120.
- Patya, M., Zahalka, M. A., Vanichkin, A., Rabinkov, A., Miron, T., Mirelman, D., Wilchek, M., Lander, H. M., and Novogrodsky, A. (2004) Allicin stimulates lymphocytes and elicits an antitumor effect: a possible role of p21ras, *16* 2, 275-281.
- Pizzimenti, S., Toaldo, C., Pettazzoni, P., Dianzani, M. U., and Barrera, G. (2010) The "Two-Faced" Effects of Reactive Oxygen Species and the Lipid Peroxidation Product 4-Hydroxynonenal in the Hallmarks of Cancer, *Cancers* 2, 338-363.

- Shah, A., Stiller, C. A., Kenward, M. G., Vincent, T., Eden, T. O. B., and Coleman, M. P. (2008) Childhood leukaemia: long-term excess mortality and the proportion 'cured', *British Journal of Cancer* 99, 219-223.
- Silva, M. T. (2010) Secondary necrosis: The natural outcome of the complete apoptotic program, *Federation of European Biochemical Societies Letters* 823, 4150-4180.
- Singh, B. N., Singh, B. R., Singh, R. L., Prakash, D., Dhakarey, R., Upadhyay, G., and Singh, H. B. (2009) Oxidative DNA damage protective activity, antioxidant and anti-quorum sensing potentials of *Moringa oleifera*, *Food and Chemical Toxicology* 47, 1109–1116.
- Singh, N. P., McCoy, M. T., Tice, R. R., and Schneider, E. L. (1988) A simple technique for quantitation of low levels of DNA damage in individual cells, *Experimental Cell Research* 175, 184–191.
- Sinks, L. F. (1972) Treatment of Acute Lymphoblastic Leukaemia, *Archives of Disease in Childhood* 47, 811-813.
- Sompayrac, L. (2008) *How the immune system works*, Third Edition ed., Blackwell Publishing.
- Stefan, D., C, and Stones, D. K. (2012) The South African Paediatric Tumour Registry – 25 years of activity, *South African Medical Journal* 102.
- Tang, W., Liu, Q., Wang, X., Wang, P., Cao, B., Mi, N., and Zhang, J. (2008) Involvement of Caspase 8 in Apoptosis Induced by Ultrasound-Activated

Hematoporphyrin in Sarcoma 180 Cells In Vitro, *Journal of Ultrasound and Medicine* 27, 645–656.

Tarpey, M. M., Wink, D. A., and Grisham, M. B. (2004) Methods for detection of reactive metabolites of oxygen and nitrogen: in vitro and in vivo considerations, *American Journal of Physiology - Regulatory, Integrative and Comparative Physiology* 286, 431-444.

Thannickal, V. J., and Fanburg, B. L. (2000) Reactive oxygen species in cell signaling, *American Journal of Physiology - Lung Cellular and Molecular Physiology* 279, 1005-1028.

Tudek, B., Winczura, A., Janik, J., Siomek, A., Foksinski, M., and Oliński, R. (2010) Involvement of oxidatively damaged DNA and repair in cancer development and aging, *American Journal of Translational Research* 2, 254-284.

Turrens, J. F. (2003) Mitochondrial formation of reactive oxygen species, *Journal of Physiology* 552, 335-344.

Ushmorov, A., Ratter, F., Lehmann, V., Droge, W., Schirmmacher, V., and Umansky, V. (1999) Nitric Oxide–Induced Apoptosis in Human Leukemic Lines Requires Mitochondrial Lipid Degradation and Cytochrome C Release, *Blood* 93, 2342-2352.

Valko, M., Leibfritz, D., Moncola, J., Cronin, M. T. D., Mazura, M., and Telser, J. (2007) Free radicals and antioxidants in normal physiological functions and human disease, *The International Journal of Biochemistry & Cell Biology* 39, 44-84.

- Van Meerloo, J., Kaspers, G. J. L., and Cloos, J. (2011) Cell Sensitivity Assays: The MTT Assay, *Methods in Molecular Biology* 731, 237-245.
- Verhoef, M. J., Rose, M. S., White, M., and Balneaves, L. G. (2008) Declining conventional cancer treatment and using complementary and alternative medicine: a problem or a challenge?, *Integrative Oncology* 15, S31-S36.
- Vermes, I., Haanen, C., Steffens-Nakken, H., and Reutelingsperger, C. (1995) A novel assay for apoptosis. Flow cytometric detection of phosphatidylserine expression on early apoptotic cells using fluorescein labelled Annexin V, *Journal of Immunological Methods* 184, 39-51.
- Vistica, D. T., Skehan, P., and Scudiero, D. (1991) Tetrazolium-based Assays for Cellular Viability: A Critical Examination of Selected Parameters Affecting Formazan Production, *Cancer Research* 51, 2515-2520.
- Walker, L. M., York, J. L., Imam, S. Z., Ali, S. F., Muldrew, K. L., and Mayeux, P. R. (2001) Oxidative Stress and Reactive Nitrogen Species Generation during Renal Ischemia, *Toxicological Sciences* 63, 143–148.
- Wang, H., Jiang, M., Cui, H., Chen, M., Buttyan, R., Hayward, S. W., Hai, T., Wang, Z., and Yan, C. (2012) The stress response mediator ATF3 represses androgen signaling by binding the androgen receptor., *Molecular and Cellular Biology* 32, 3190-3202.
- Waris, G., and Ahsan, H. (2006) Reactive oxygen species: Role in the development of cancer and various chronic conditions, *Journal of Carcinogenesis* 5, 1-8.

- Wu, G., Fang, Y., Yang, S., Lupton, J. R., and Turner, N. D. (2004) Glutathione Metabolism and Its Implications for Health, *The Journal of Nutrition* 134, 489–492.
- Zaid, H., Silbermann, M., Ben-Arye, E., and Saad, B. (2011) Greco-Arab and Islamic Herbal-Derived Anticancer Modalities: From Tradition to Molecular Mechanisms, *Evidence-Based Complementary and Alternative Medicine* 2012, 1-13.
- Zhang, W. L. (2011) The role of inflammation in breast cancer and prostate cancer, *Clinical Oncology Cancer Research* 8, 77-84.
- Zong, W., and Thompson, C. B. (2006) Necrotic death as a cell fate, *Genes and Development* 20, 1-15.

APPENDICES

APPENDIX A

TBARS ASSAY REAGENT PREPARATIONS

- i. TBA/BHT - 250 μ l of 20mM BHT stock solution was dissolved in 40ml dH₂O, and then mixed until dissolved. This solution was then topped up to 50ml with dH₂O.
- ii. Positive control – 1 μ l MDA
- iii. Negative control – 100 μ l complete culture medium (CCM).

APPENDIX B**NITRIC OXIDE ASSAY REAGENT PREPARATION**

- i. VCl₃ – 100mg of VCl₃ was dissolved in 12.5ml of 1M HCl and filter sterilized. Reagent was kept in foil and in dark at 4°C.
- ii. NEDD – 10mg NEDD was dissolved in 10ml dH₂O.
- iii. SULF – 200mg SULF was dissolved in 10ml of 5% HCl (3ml 1MHCl +15ml dH₂O) and stirred on a hot plate. Reagent was kept in foil and in the dark at 4°C.
- iv. Standards – 6.06mg Sodium Nitrite was dissolved in 30ml dH₂O and 200 μM stock was made up to 10 standards ranging from 0 μM - 200 μM.

APPENDIX C

SCGE ASSAY REAGENT PREPARATION

- i. Phosphate Buffer Saline (0.1M PBS) –
Stock A: 0.2M Sodium dihydrogen orthophosphate (dissolve 6.24g in 200ml dH₂O).
Stock B: 0.2M diSodium hydrogen orthophosphate (dissolve 11.32g in 400ml dH₂O).
Stock C: 1M Sodium Chloride (dissolve 4.25g in 500ml dH₂O).
This was prepared by mixing 160ml stock A, 340ml stock B, and 500ml stock C. The pH was then adjusted to 7.4.
- ii. . 0.5 % and 1% LMPA - 0.5 % and 1% LMPA was prepared by dissolving 0.5g and 1g LMPA in 100ml PBS respectively.
- iii. Cell lysis buffer (Lysing solution) – this was made by dissolving 36.5g 2.5M Sodium Chloride (NaCl) and 7.3g 100mM EDTA in 200ml dH₂O. Next, 2.5ml 1% Triton X was added, followed by 2.5ml 1M Tris and 25ml 10% dimethyl sulphoxide (DMSO). This mixture was then stirred, and then topped up to 500ml with dH₂O.
- iv. Alkaline electrophoresis tank buffer – 12g sodium hydroxide (NaOH) and 0.372g Na₂EDTA was dissolved in 800ml dH₂O. The pH was then adjusted to pH 7.4, and the mixture topped up to 1000ml with dH₂O.
- v. Neutralisation buffer (0.4M Tris; pH 7.4) – 48.46g Tris was dissolved in 800ml dH₂O, and the mixture adjusted to a pH of 7.4. This was then topped up to 1000ml.

APPENDIX D

DNA FRAGMENTATION GEL PREPARATION

- i. Cell lysis solution - 0.5M EDTA stock (pH 8.0) was prepared by adding 186.1g EDTA to 800ml dH₂O. The pH was then adjusted to pH 8 and the solution topped up to top to 1L. Next, 100 μ l 0.5M EDTA, 500 μ l Tris-Cl and 0.5g 0.1% SDS were mixed together. This was then topped up to 50ml.
- ii. Potassium acetate buffer - 5M Potassium acetate (60ml (29.45g in 60ml dH₂O)) was mixed with 11.5ml Glacial Acetic Acid, followed by the addition of 28.5ml dH₂O.
- iii. 10 x TE buffer - 10mM EDTA (pH 8) (1ml) was added to 5ml 100mM Tris-Cl (pH 7.4), and then topped up to 50ml with dH₂O.
- iv. 5x TBE buffer- Tris (108g), Boric acid (55g) and 0.5M EDTA (40ml) were all mixed together and then dissolved in 800ml dH₂O. This mixture was then topped to 1L and covered with foil (light sensitive).
- v. Loading dye- Bromophenol blue (25mg) and sucrose (4g) were dissolved in 10ml dH₂O.
- vi. 1.8% gel - Dissolve 1.8g of Agarose powder in 100ml 1 x TBE buffer. This solution was heated and mixed until clear. Ethidium bromide (2 μ l) was then added.
- vii. 2% gel - Dissolve 2g of Agarose powder in 100ml 1 x TBE buffer. This solution was heated and mixed until clear. Ethidium bromide (2 μ l) was then added.

APPENDIX E**JC-1 REAGENT PREPARATION**

- i. JC-1 stock solution - Reconstitute the JC-1 reagent at room temperature with 125 μ l DMSO (per vial) and then invert several times.
- ii. JC-1 working solution - Dilute the JC-1 Stock Solution 1:100 with pre-warmed 1 x Assay Buffer. Vortex the solution and then use immediately.

APPENDIX F**WESTERN BLOT REAGENT PREPARATION**

- i. 1X Tank running buffer – 100ml 10X SDS running buffer (30.3g Tris+144g Glycine + 10g SDS dissolved in 800ml dH₂O) was diluted with 900ml dH₂O. This was then placed in the fridge and left to cool.
- ii. Transfer buffer – 8ml 10X transfer buffer (3.03g Tris + 14.4g Glycine + 200ml methanol dissolved in 600ml dH₂O) was added to 720ml dH₂O and 200ml methanol. This was then placed in the fridge and left to cool.
- iii. TTBS wash buffer – 100ml 10X TTBS wash buffer (8g NaCl +0.2g KCl + 3g Tris dissolved in 800ml dH₂O + 500µl tween 20) was diluted with 500ml dH₂O. This was then adjusted to pH 7.4. Next, 400ml dH₂O and 500µl Tween 20 were added. This was then mixed and then placed in the fridge to cool.
- iv. BSA standards were prepared by making a 1mg/ml stock solution by dissolving 1mg BSA in 1ml dH₂O. This was then diluted 6 times with dH₂O. The standards that were prepared included the following concentrations – 0, 0.2, 0.4, 0.6, 0.8 and 1mg/ml
- v. 2% BSA- 1g BSA was dissolved in 50ml TTBS wash buffer and then placed in the fridge to cool.
- vi. 7.5% resolving gel- For 1 gel, the following was mixed together – 2.5ml 30% Bis, 2.5ml 1.5M Tris HCl 8.8, 0.1ml 10% SDS, 4.85ml dH₂O, and lastly, 5µl TEMED and 50 µl 10% APS was added. The SDS plates were set up, and the resolving gel mixture was poured in and allowed to polymerase for 40 minutes.
- vii. 4% stacking gel- For 1 gel, the following was mixed together – 0.33ml 30% Bis, 0.63ml 1.5M Tris HCl 8.8, 25 µl 10% SDS, 1.5ml dH₂O, and lastly, 2.5µl

TEMED and 2.5 μ l 10% APS was added. This mixture was added on top of the pre set resolving gel. Combs were placed into the setting gel mixture to create lanes. This was then allowed to polymerase for 40 minutes.

APPENDIX G**REAGENT PREPARATION FOR COOMASIE BLUE STAINING**

- i. Coomassie blue stain – 1% coomassie blue stock (1g coomassie blue R250 dissolved in 100ml dH₂O)(62.50ml) was mixed with 250ml methanol and 50ml acetic acid, and then topped up to 500ml with dH₂O.
- ii. Destaining 1 – 400ml methanol was added to 100ml acetic acid and then topped up to 1l with dH₂O.
- iii. Destaining 2 – 70ml methanol was added to 100ml acetic acid and then topped up to 1l with dH₂O.

APPENDIX H

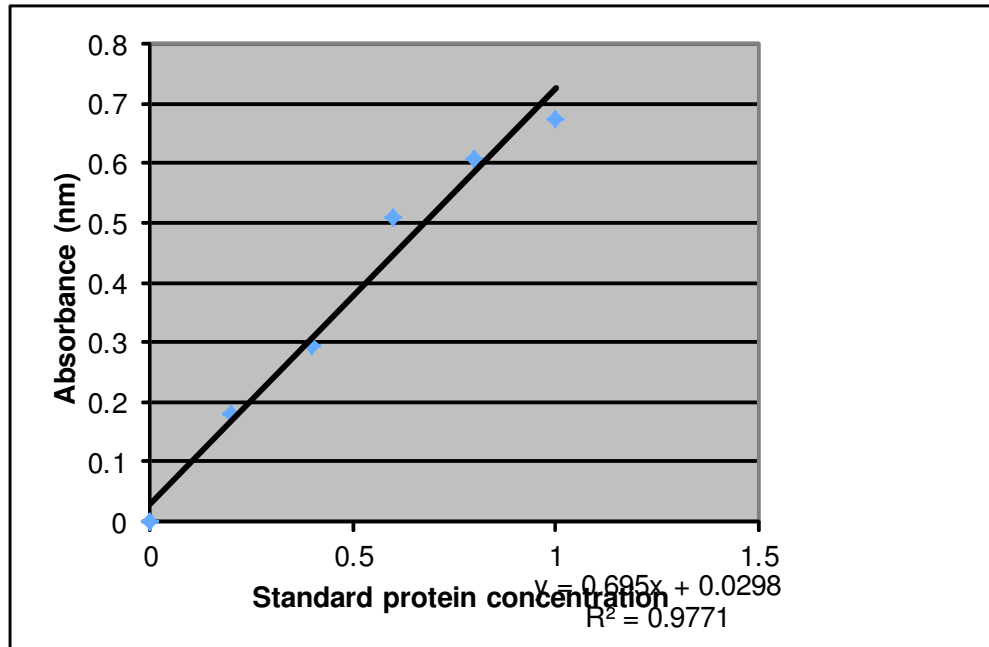


Figure 22: Standard curve used in order to determine and standardise protein concentration in western blots

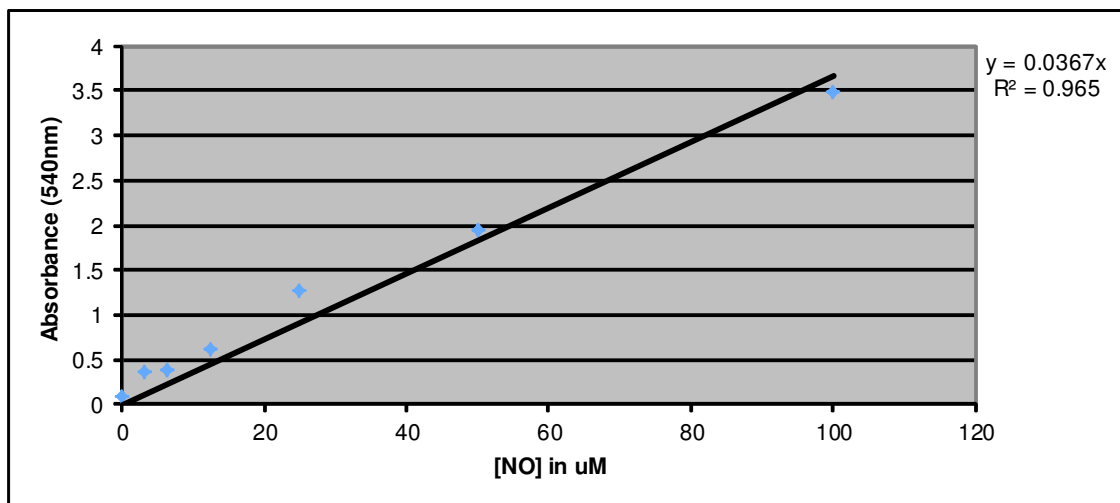


Figure 23: Standard curve used to determine NO concentration.

Table 4: Individual comet visual scores following an SCGE assay.

	Control	Garlic	TV Leaf	TV Bulb	TV Stalk
1	0	3	1	3	3
2	0	3	1	3	3
3	1	3	2	3	3
4	0	4	2	3	3
5	0	3	2	3	2
6	0	3	1	3	2
7	0	3	1	3	2
8	1	3	1	4	1
9	1	3	4	3	2
10	0	4	3	3	2
11	0	4	3	3	3
12	0	4	2	3	3
13	0	3	2	3	3
14	0	2	2	3	3
15	0	2	2	3	3
16	0	3	2	4	3
17	1	3	3	4	2
18	0	2	3	3	2
19	0	3	3	3	3
20	0	3	3	3	3
21	0	2	3	3	3
22	0	2	2	3	3
23	0	2	3	4	3
24	0	2	3	4	3
25	1	3	3	3	3
26	0	3	3	3	3
27	0	3	3	2	3
28	0	4	3	3	3
29	0	1	3	3	3
30	0	1	3	3	3
31	0	1	3	3	3
32	0	3	4	3	4
33	0	3	3	4	3
34	0	3	3	4	3
35	0	3	3	3	3
36	0	4	4	3	3
37	1	2	3	3	3
38	0	2	3	3	4
39	0	3	3	3	3
40	0	3	3	3	3
41	0	3	2	3	3
42	4	3	2	3	2
43	0	2	1	3	2
44	0	2	1	3	2
45	0	2	2	4	2
46	1	3	2	3	2
47	0	3	2	3	2
48	0	3	3	3	3
49	0	4	2	3	3
50	0	4	2	3	3
Total visual Score	11	140	123	157	137

RELATIVE BAND DENSITY

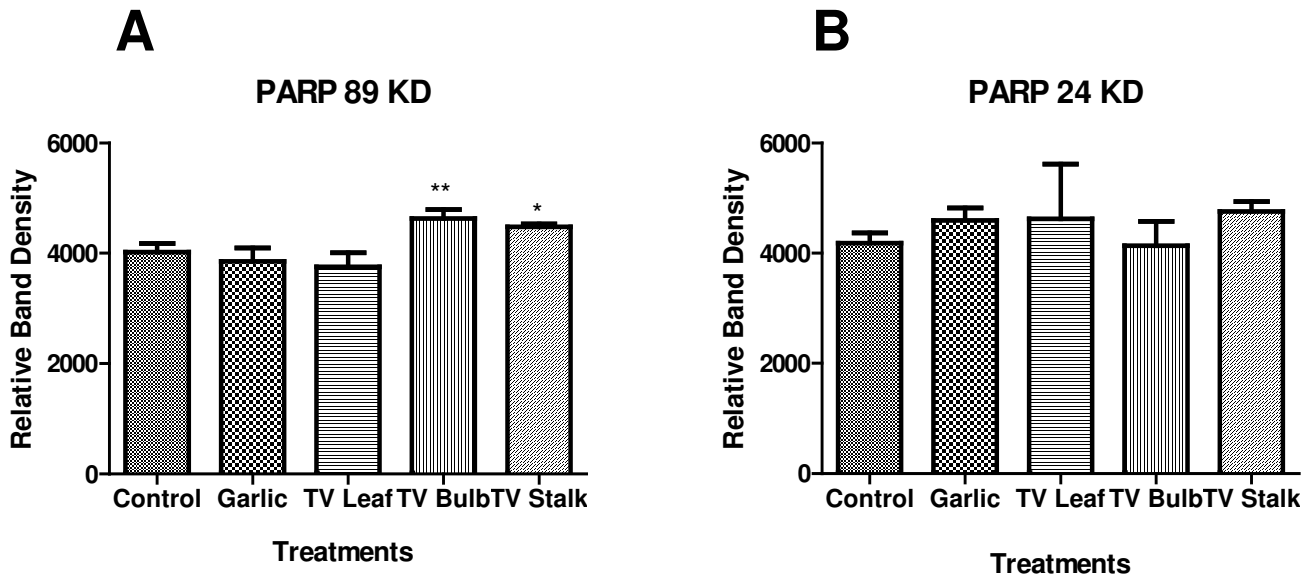


Figure 24: Relative Band Density for all treatments, including the control, after performing a western blot analysis. A) PARP 89 KD, and B) PARP 24 KD. Values are presented as Means \pm SD, where the columns represent means, and the vertical lines represent SD. * $p < 0.05$ and ** $p < 0.001$ by comparison with the control group.

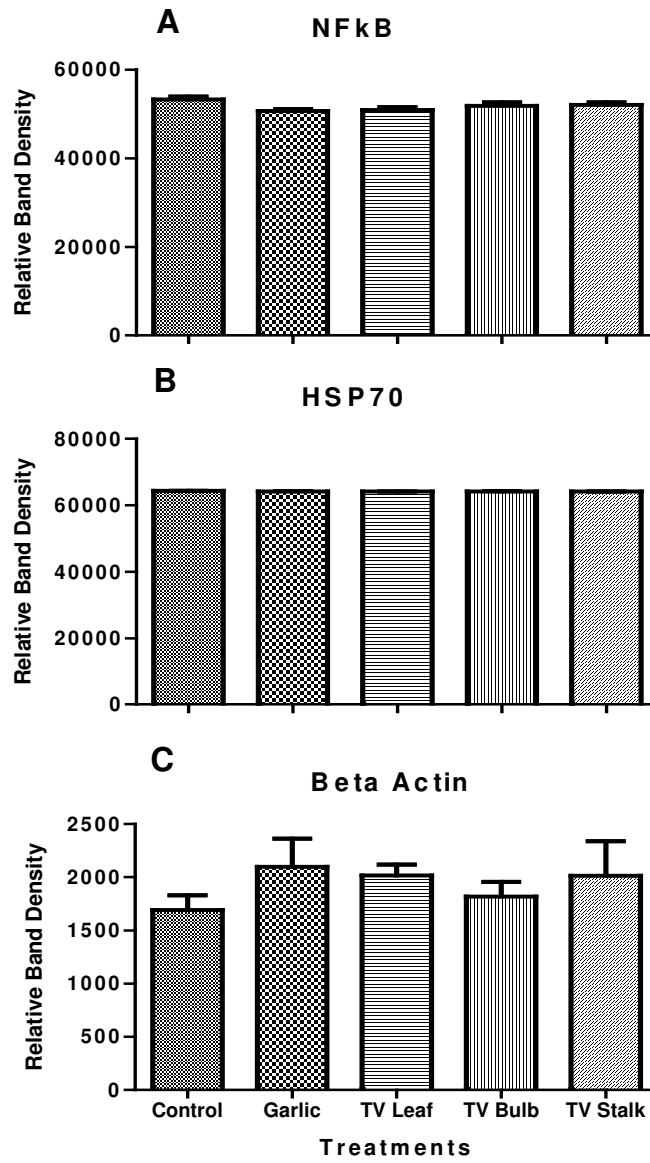


Figure 25: Relative Band Density for all treatments, including the control, after performing a western blot analysis. A) NFκB, B) HSP 70, and C) Beta actin. Values are presented as Means \pm SD, where the columns represent means, and the vertical lines represent SD.

